



# **Development of an in-line measuring tool for ribbon solid fraction during roll compaction**

Inaugural-Dissertation

zur Erlangung des Doktorgrades

der Mathematisch-Naturwissenschaftlichen Fakultät

der Heinrich-Heine-Universität

vorgelegt von

Raphael Wiedey

aus Greven

Düsseldorf, Juli 2018

aus dem Institut für Pharmazeutische Technologie und Biopharmazie  
der Heinrich-Heine-Universität Düsseldorf

Gedruckt mit der Genehmigung der  
Mathematisch-Naturwissenschaftlichen Fakultät der  
Heinrich-Heine-Universität Düsseldorf

Berichtersteller:

1. Prof. Dr. Dr. h.c. Peter Kleinebudde
2. Prof. Dr. Jörg Breitzkreutz

Tag der mündlichen Prüfung: 04.09.2018

## Table of contents

1	Introduction .....	1
1.1	Roll compaction/dry granulation .....	1
1.1.1	General.....	1
1.1.2	Ribbon solid fraction in roll compaction/dry granulation .....	5
1.1.3	Ribbon homogeneity in roll compaction/dry granulation.....	8
1.1.4	PAT in roll compaction/dry granulation.....	10
1.2	X-ray micro-computed tomography .....	13
1.2.1	General.....	13
1.2.2	Pharmaceutical applications .....	15
1.3	Infrared thermography .....	17
1.3.1	General.....	17
1.3.2	Pharmaceutical applications .....	19
1.4	Aims of the thesis.....	20
1.5	Outline of the thesis .....	21
2	The density distribution in ribbons from roll compaction.....	31
2.1	Pretext .....	31
3	How relevant is ribbon homogeneity in roll compaction/dry granulation and can it be influenced? .....	33
3.1	Pretext .....	33
4	Infrared Thermography - A new approach for in-line density measurement of ribbons produced from roll compaction .....	35
4.1	Pretext .....	35
5	Potentials and limitations of thermography as an in-line tool for determining ribbon solid fraction .....	37
5.1	Pretext .....	37
6	Laser based thermo-conductometry as an approach to determine ribbon solid fraction off-line and in-line.....	39

6.1	Pretext .....	39
7	Summary and outlook .....	41
8	Zusammenfassung und Ausblick .....	47
9	List of original publications .....	54
10	Contributions to meetings .....	55
10.1	Oral presentations .....	55
10.2	Poster presentations .....	55
11	Danksagung .....	56
12	Appendix .....	58
12.1	General .....	58
12.2	Averaging images .....	58
12.3	Gaussian fit row-wise .....	59
12.4	Plotting $\sigma$ and amplitude of peaks .....	61

## List of abbreviations

API	active pharmaceutical ingredient
BCS	Biopharmaceutical Classification System
CCD	charge-coupled device
CP	cheek plates
CV	coefficient of variation
DCPA	dibasic calcium phosphate anhydrate
EMA	European Medicines Agency
FDA	United States Food and Drug Administration
GSD	granule size distribution
GW	gap width
MCC	microcrystalline cellulose
MgSt	magnesium stearate
NIR	near-infrared
PAT	Process Analytical Technology
RCDG	roll compaction/dry granulation
RR	rim rolls
SCF	specific compaction force
X $\mu$ CT	X-ray micro-computed tomography



# 1 Introduction

## 1.1 Roll compaction/dry granulation

### 1.1.1 General

Granulation is an important process step in the manufacturing of many pharmaceutical dosage forms. During granulation, particles are agglomerated to larger entities called granules. The main motivations for this are an increased flowability, higher bulk density, dust reduction, a decreased tendency for separation, and in some cases solubility enhancement. Flowability depends mainly on the ratio between gravitational force and cohesive forces. Since gravitational force is proportional to particle mass while cohesive forces are proportional to particle surface, larger particles show a higher ratio between the forces and hence a better flowability. Particle separation is reduced, because particles of all components are connected and by that fixed in homogeneously composed agglomerates. Even though granules can represent a pharmaceutical dosage form on their own, they are in most cases intermediate products for subsequent processing.

One of the ways to categorize the several granulation techniques is by the presence of granulation liquid during the process. During wet granulation, an aqueous or organic liquid is present, which is subsequently evaporated during a drying step. Binders or other excipients dissolved in the liquid solidify during this drying step and form connecting bridges between the particles. Melt granulation represents a special case, as the granulation liquid is solid at room temperature, melted during granulation, and afterwards not evaporated but solidified during cooling. During dry granulation however, no liquids are present and the particle cohesion is mostly caused by van der Waals forces. Powder is compressed to a large compact and afterwards milled to granules. The compression can be performed on tablet machines using large punches. This approach, called slugging, is problematic in several ways. The production capacity is low, control over compression pressure is limited, and lubrication of the powder is needed [1-3]. Regarding all those factors, dry granulation by roll compaction is superior. During roll compaction, powders are compressed between counter-rotating rolls. The resulting compacts are called ribbons or flakes. Commercially available roll compactors are set up in three units (Figure 1-1). The feeding unit consists of a hopper for the starting material and two augers that transport powder to the compaction unit. The feeding auger doses the powder, i.e. the rotation speed

of this auger determines the amount of powder that is processed. Subsequently, the powder is fed between counter-rotating rolls by a tamping auger. In modern roll compactors, as were used in this work, one of the rolls is fixed (master roll), while the other (slave roll) is mounted on a flexible axis and applies pressure onto the powder.

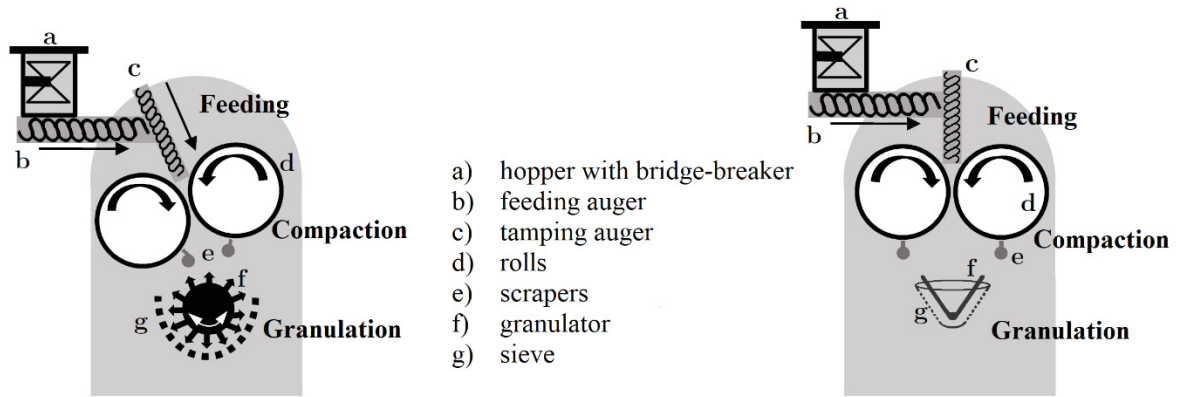


Figure 1-1: Schematic set-up of roll compactors used this work, left: MiniPactor (Gerteis, CH), right: BRC25 (L.B. Bohle, D), modified from Mosig [4]

Three different arrangements of rolls are possible in the roll compactors of different distributors. They can be arranged horizontally, inclinedly, or vertically [5]. The roll compactors used in this work had inclined or horizontal set-ups (Figure 1-1). Since in both set-ups, the powder feeding is located above the compaction unit, a gravity driven leakage of non-compacted powder is possible.

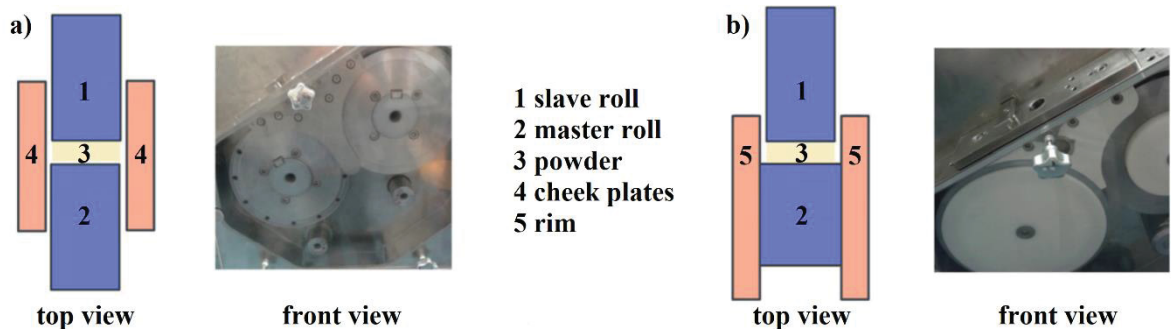


Figure 1-2: Possible side seal assemblies a) cheek plates and b) rim roll, exemplarily shown for a Gerteis MiniPactor, modified from Mazor et al. [6]

Such leakage increases the fraction of fines in the resulting granules and causes an undesirable broad granule size distribution. To avoid powder leakage, sealing systems are applied that restrict the compaction zone to the sides. Commonly used systems are the cheek plate sealing system and the application of rim rolls (Figure 1-2). Cheek plates are large static plates that are attached to the feeding unit and do not move during production.

In rim rolls however, the sealing (rim) is attached to the master roll and hence is not static but following the rotation of the rolls. The relevance of sealing systems for the compaction process and the resulting product is described in section 1.1.3. In the compaction unit, the powder is compacted to ribbons or flakes, depending on the compaction behavior of the material. These intermediate products are removed from the rolls by scrapers and fall into the granulation unit and are milled to granules. Also for the granulation unit several designs are possible. In this work, an oscillating star granulator with a mesh sieve as well as conical granulator with a rasp sieve were used (Figure 1-1).

The granules produced by roll compaction/dry granulation (RCDG) are in many ways inferior to granules produced by the various wet granulation techniques. The granule size distribution is broader with a high fraction of fines. Consequently, the flowability is usually worse. This is furthermore intensified by the irregular shape of dry granules. Wet granules on the other hand are, depending on the granulation technique, usually more spherical. Further downsides of dry granulation are the tendency of dust formation and the lacking potential of solubility enhancement. The latter one is especially important as most new active pharmaceutical ingredients (APIs) are poorly soluble and classified as class II or IV in the biopharmaceutical classification system (BCS) [7].

The downside that has been discussed most extensively in literature is the reduced tableability of dry granules. It was first observed by Malkowska and Khan that tablets compressed from dry granules showed lower tensile strengths than those produced by direct compression [8]. This effect was dependent on the pressure applied during the first compaction step. The authors attributed this observation to *work hardening*, an increased resistance of granules towards re-compression. Sun and Himmelspach criticized this explanation and hypothesized that reduced tableability of dry granules is solely caused by particle enlargement during granulation [9]. This increased particle size means also that a decreased surface area is available for bonding. Their conclusion that work hardening does therefore not contribute to the loss in tableability was criticized by Herting and Kleinebudde [10, 11]. It was laid out that the phenomenon of *work hardening* as well as particle enlargement contribute to loss in tableability after RCDG. *Work hardening* can be investigated in isolated form by comparing tableability of identical sieve cuts from granules produced at different compaction pressures [12, 13].

Despite those severe downsides, dry granulation by roll compaction has gained increased attention in pharmaceutical research as well as in pharmaceutical industry. The newly acquired status of RCDG can well be illustrated by the listing as the granulation technique of choice in a recent proposal for a *Manufacturing Classification System* [14]. The reason for this growing interest is mainly the high energy efficiency of this process. Drying is oftentimes the most energy consuming step during pharmaceutical manufacturing. The absence of any drying steps makes RCDG superior to other granulation techniques in economic and ecologic ways. All ways to generate electric energy have a negative effect on the environment, and as all large industries, also pharmaceutical industry has to face a responsibility in this regard. With increasing energy prices, energy efficient manufacturing has become an economic imperative as well. Compared to other granulation techniques, RCDG is also a time-efficient process.

A further advantage is the possibility to implement RCDG in continuous manufacturing lines [15]. The RCDG process is per se continuous, as all process steps work continuously and the batch size is only limited by process time. The main motivations for continuous manufacturing are laid out in literature as increased economic efficiency, a reduction of the ecological footprint, easy scale-up, and also increased drug product quality [16-18]. Even if not conducted in continuous manufacturing, scale-up of RCDG processes is unproblematic, as the batch size can be increased by longer process times. Furthermore, roll compactors of different scale (from the same distributor) usually differ in their roll width, while the roll diameter is identical. Hence, also the physical conditions during compaction are identical and process parameters can be transferred.

The most relevant process parameters during the compaction step are the compaction pressure, the gap width, and the roll speed. Pressure is the force divided by the surface on which the force is applied. This surface can hardly be quantified, as it is not confined along the roll circumference. Hence, the compaction force is usually standardized only regarding the roll width and called specific compaction force (SCF). The resulting unit is kN/cm. While some manufacturers also use the hydraulic pressure as a process parameter, the roll compactors used in this work use the specific compaction force. The influence of process parameters on the resulting product is described in section 1.1.2.

A detailed model describing the compaction process was given by Johanson [19]. It describes the applied pressure and nip angle in dependence from roll diameter, friction, gap

width, and feed pressure. Alternative models are given in form of the thin layer model by Peter et al. [20], as well as by discrete element [21] and neuronal network modeling [22, 23]. Generally, the space between the rolls is divided into three zones (Figure 1-3). In the feeding zone (I), the forces applied on the powder are low and densification occurs only as a result of particle rearrangement. The compaction zone (II) is defined as the region in which friction between powder and roll is sufficiently high to cause directive transport towards the gap and compaction forces induce plastic deformation or particle breaking. The angle between roll gap, roll center, and edge of the compaction zone is the nip angle  $\alpha$  [5]. In the extrusion zone (III), the freshly formed compacts leave the gap and elastic recovery can occur. If friction between powder and roll is insufficient, the nip angle is reduced and so is the degree of densification. This can be improved by application of rolls with rough or knurled surface, which cause increased friction.

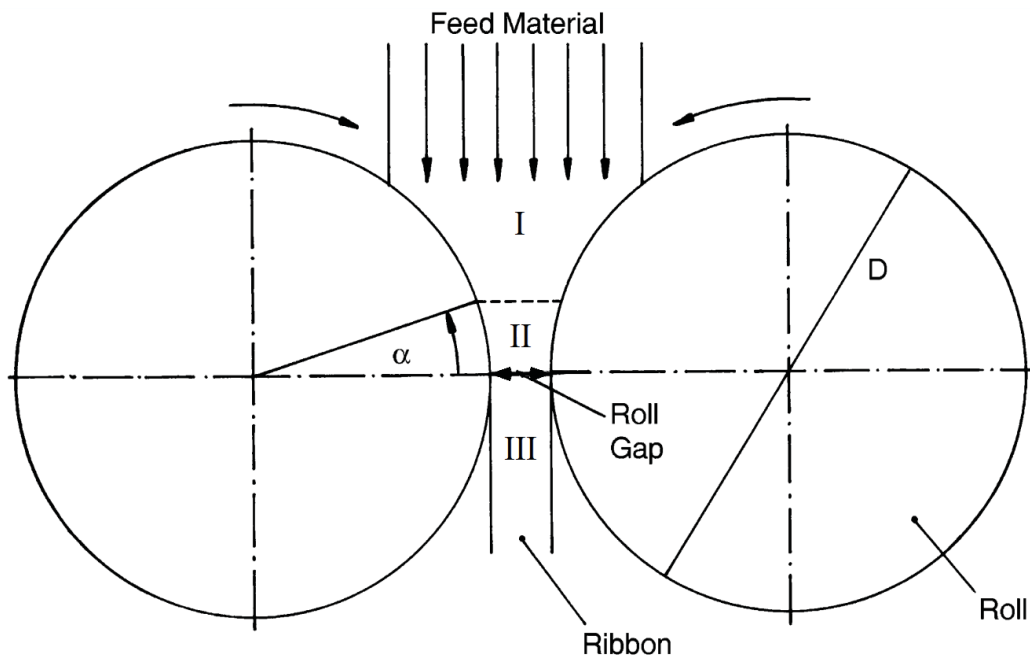


Figure 1-3: Zones in between rolls: I, feeding zone; II, compaction zone; III, extrusion zone;  $\alpha$ , nip angle; D, roll diameter, modified from Kleinebudde [3]

### 1.1.2 Ribbon solid fraction in roll compaction/dry granulation

The most critical quality attributes during RCDG are granule size distribution (GSD) and granule solid fraction. GSD is important, because it predominantly determines the flowability of granules, which is key for volumetric dosing of tablets, capsules, and other dosage forms [24, 25]. Granule solid fraction is critical, because it influences the properties of resulting tablets. It can affect the compactability [26] as well as disintegration and dissolution behavior [27]. Also the phenomenon of *work hardening*, that was described in

section 1.1.1, is usually attributed to the loss in material porosity during the first compaction step [8, 28]. Solid fraction is defined as the ratio between envelope density ( $\rho_{env}$ ) and true density ( $\rho_{true}$ ) or particle density (Equation 1). In literature, oftentimes the terms relative density, which is in this field used synonymously, or the complementary dimension porosity ( $\varepsilon$ ) are used.

$$solid\ fraction = \frac{\rho_{env}}{\rho_{true}} = 1 - \varepsilon \quad (1)$$

Both characteristics, GSD and granule solid fraction, are predominantly determined by ribbon solid fraction. The connection between solid fraction after the first compaction step and GSD was first observed by Jaminet and Hess [29]. In their set-up, the compaction force could not be controlled directly, but indirectly by the ratio of auger speed and roll speed. At higher ratios – and by that higher compaction force – larger granules with a smaller fraction of fines were produced. Their findings have been confirmed many times in literature for a wide range of materials. Naturally, also the dimensions of the sieves used for milling/granulation affect the GSD. Mangal et al. have demonstrated that furthermore the granulator settings, namely the impeller speed, have an effect on GSD, but also in their study, the influence of SCF dominated [30].

The relevance of ribbon solid fraction for granule solid fraction is based on the common assumption that solid fraction is conserved during the milling process. Since it is experimentally challenging to determine granule solid fraction, especially if those granules show a broad GSD [31], as dry granules usually do, ribbon solid fraction is often used as a surrogate for granule solid fraction.

Despite the high relevance of ribbon solid fraction, no measurement technique is available that is generally accepted to give accurate and precise results. The solid fraction is a composite measure, based on the true density and the envelope density. True density is usually approximated by helium pycnometry, while the envelope density can be determined by other pycnometric techniques, namely mercury pycnometry and powder pycnometry. Pycnometers are devices to determine volumes. To calculate the corresponding density, the sample weight has to be determined separately. Due to the high toxicological potential of mercury, powder pycnometry is the method of choice in many publications [32, 33]. In both cases, a sample chamber of defined volume is filled with a non-compressible medium. This is done once with and once without the sample and the difference in overall volume

determined. Both techniques have the downside that voids or cracks that regularly appear in ribbons (*lamination*), cannot be accessed by the medium. In these cases, the measuring results for density as well as solid fraction are systematically underestimated. Also the precision is limited and the coefficient of variation in literature usually ranges between 1 and 4 % [32-35].

Another method regularly used in this field is the oil absorption technique [36, 37]. For this, the samples are weighed, placed in liquid paraffin so that pores are saturated, and subsequently weighed again. This approach has the advantage of minimal instrumental effort, but is highly time consuming and also susceptible to systematic errors in case of laminating ribbons. The same is the case for a laser-based scanning of the outer geometry of ribbons that is used increasingly in pharmaceutical research and development [38, 39]. It is equally prone to underestimation of solid fraction in presence of voids and gaps. Since it only determines the sample volume, the samples have to be collected and weighed, making the solid fraction determination relatively time consuming, despite short measurement times of the laser set-up itself. A further limitation is that the smallest measurable ribbon thickness is 1.0 mm, which could sometimes not be reached if the powder does not form intact ribbons, but rather flakes [40].

X-ray micro-computed tomography ( $X\mu$ CT) has been used in two different ways to determine ribbon solid fraction. In some studies, tomographic images of high resolution were obtained, digitally binarized, and the solid fraction derived [41-43]. The downside of this approach is that only pores larger than a certain size are detectable. This limit depends on the voxel size of the CT image. As a rule of thumb, pores are detectable with satisfactory certainty if they have a volume of  $3 \times 3 \times 3$  voxels or larger [44, 45]. Since the achievable voxel size in a  $X\mu$ CT measurement is linked to the sample size (as is laid out in more detail in section 1.2.1), these measurements have only been performed on fragments of ribbons. This is problematic, because single fragments of ribbons might not be representative for the whole ribbon, as is described in section 1.1.3. The second approach was introduced by Miguélez-Morán and works with measurements performed with lower resolution ( $\cong$  larger voxel size) [46]. In those studies, the voxels were too large to isolate pores and solids via binarization. Instead, a mean gray value over the ribbon is calculated. Additionally, a stack of calibration tablets of the same material and known solid fraction is measured. As laid out in section 1.2.1, the gray value is proportional to the sample density. Hence, the correlation of gray value and solid fraction can be used for calibration and the mean gray

value of the ribbon can be transferred to solid fraction. This works also for larger samples and ribbons can be analyzed in their entirety.

Spectroscopic measurements have been used in a broad range of pharmaceutical applications and some techniques are also suitable to determine ribbon solid fraction. Especially near-infrared (NIR) spectroscopy has been used for this [36, 37, 47, 48]. The reflection spectra are influenced not only by the chemical composition (including moisture), but also by the solid fraction [49]. Another suitable method is Terahertz spectroscopy, which additionally allows pore size and pore structure analysis [50]. The application of NIR and Terahertz spectroscopy on solid fraction measurements of ribbons is described in more detail in section 1.1.4.

### **1.1.3 Ribbon homogeneity in roll compaction/dry granulation**

It is well described in literature that solid fraction is not homogeneous within the ribbon. Inhomogeneity was observed especially across the ribbon width. Already in the 1970's, Funakoshi et al. reported an uneven distribution of ribbon hardness, which was used as a surrogate for solid fraction [51]. In their study and several others, it was found that the solid fraction in the center of the ribbon is different than it is near the edges. Techniques for measuring the density distribution in literature are the determination of surrogate parameters like the force needed for drilling at different positions [51], cutting the ribbon in pieces and determining the solid fraction of each piece [41, 48], X $\mu$ CT [46, 52], NIR chemical imaging, and ultrasonic imaging [52]. The detailed distribution depends on the sealing system that was used during roll compaction. If cheek plates are used, the center of the ribbon shows the highest solid fraction, while the edges are more porous [46, 51, 53]. If however rim rolls are used, the distribution is more homogeneous with slightly increased solid fraction near the edges [54, 55]. The cause of this inhomogeneity is friction between powder and the sealing plates, as was laid out by Parrot [1]. At the border between feeding and compaction zone, the powder is transported by the rolls but slowed down by the static plate. Hence, less material is transported to the gap near the edges where the sealing plates are located and the resulting solid fraction is reduced. If rim rolls are used, the sealing plates (rims) are not static but following the rotation of the roll and no friction occurs.

Characteristic distribution patterns have been observed along the ribbon length, too. Funakoshi et al. used the addition of riboflavin, which increases in color under pressure, to visualize distribution patterns and found a sinusoidal curve of highest density along the

ribbon length [51]. Guigon measured optic light transmission through sodium chloride ribbons and linked the periodicity of the pattern to the rotation speed of the tamping auger [5]. Both authors used cheek plate sealing systems for their studies. The solid fraction patterns along the length of rim rolls ribbons have not been described in literature, yet. The reason for this is probably that ribbons produced with rim rolls are stuck between the rims after compaction and forcefully removed by the scraper. During this procedure, the ribbons usually break to pieces of a few millimeters to a few centimeters in length, making it challenging to analyze patterns of lower periodicity. Also homogeneity over the ribbon thickness has not been investigated yet, but the unidirectional character of compression during roll compaction makes an inhomogeneity over this direction plausible.

With the first publications describing inhomogeneity in ribbons came also the first efforts to increase homogeneity. The approaches were made mainly on side of the machine. Funakoshi et al. used a concavo-convex set of rolls to produce ribbons of increased homogeneity [51]. Their work was further advanced by Parrot, who stated that the main advantage of the new geometry is a reduced friction between powder and sealing plate [1]. This understanding ultimately led to the development of rimmed rolls of which the concavo-convex system can be seen as a precursor. A modification of the feeding unit was proposed by Peter et al., who installed a stirrer into the feeding zone between tamping auger and rolls [56]. They achieved an increased homogeneity in their experimental set-up, but no proceeding studies regarding this set-up have been published nor can it be found in any marketed product. In a recent study, Yu and Salman added obstacles to the feeding guiders to prohibit an accumulation of powder in the center and to guide it towards the edges instead [41]. One approach to increase ribbon homogeneity, that lays not in modification of the machine, was the observation made by Miguélez-Morán et al. that the addition of lubricants leads to higher homogeneity within ribbons [57]. It has to be considered though that negative effects linked to lubrication, i.e. weaker tablets [58] and increased disintegration and drug liberation times [59], are especially pronounced if added to a powder mixture before granulation. In addition to these negative effects on the quality of the final product, also the RCDG process is negatively affected in the way that the nip angle is decreased [57]. Even though the effect of process parameters on the overall ribbon solid fraction as well as on the GSD has been studied elaborately, their impact on ribbon homogeneity has not been described in literature, yet.

All the aforementioned efforts to increase homogeneity are based on the common assumption that more homogeneous ribbons lead to more homogeneous granules and that this homogeneity is relevant for the quality of subsequently produced dosage forms. It might be plausible that the porous regions from inhomogeneous ribbons result in higher fraction of fines, which negatively affect flowability and hence increase mass variability during tablet compression. The highly densified regions within such ribbons on the other hand could lead to granules with a high loss in tableability. However, these effects have not been studied and the relevance of ribbon homogeneity has not been discussed in literature.

### **1.1.4 PAT in roll compaction/dry granulation**

In conventional pharmaceutical manufacturing, the quality of the final product is analytically tested in an extensive way. For this, a representative sample has to be collected which is subsequently analyzed off-line, i.e. this testing is performed in a locally separated laboratory with a temporal delay [60]. Also samples from intermediate products like powder blends or granules can be collected and undergo the same procedure. In-process control is mostly performed at-line, testing a few quality characteristics that allow for timely analysis (e.g. testing of tablet mass) so control of the process is possible to a certain degree. Process Analytical Technologies (PAT) follow a different concept. They are sophisticated technologies that allow to timely monitor critical quality attributes [61]. Process Analytical Technology has become of high interest in modern pharmaceutical manufacturing. The FDA and EMA highly encourage application of PAT tools to increase process understanding and by that ensure high quality of pharmaceutical products [61, 62]. Furthermore, reduced production cycles, higher efficiency regarding energy and material use, and improved operator safety are listed by the agencies. The idea of PAT is strongly linked to the concept of continuous manufacturing. A high motivation for pharmaceutical industry to implement these two concepts is the possibility for real time release of the manufactured product and the possibility to control process parameters and by that prevent the necessity to discharge large amounts of product [15].

Since RCDG is a continuous process, the implementation of PAT tools is highly desired. The efforts to monitor the process have been focused on a number of diverse quality attributes that were deemed relevant by the respective authors. These attributes were GSD, ribbon solid fraction, and API concentration, but also breaking force/tensile strength of ribbons, Young Modulus, and moisture (as will be laid out in detail later on). Ribbon strength and Young Modulus are directly linked to ribbon solid fraction, while GSD also

depends on other process parameters. API concentration and moisture are highly important quality characteristics, but could just as well be monitored in other process steps (e.g. blending) and thus are not the primary focus during RCDG. This is especially the case for continuous processing, in which the process steps are succeeding immediately. Hence, most studies in literature that deal with PAT in RCDG focus on the ribbon solid fraction.

The first studies aiming to monitor ribbon solid fraction in-line were performed by Hakanen et al., who installed a microphone near the compaction unit and recorded the acoustic emissions occurring during compaction [63, 64]. The sound of the material during compaction was in parts at different frequencies than the sounds of the machine, making an isolated observation possible. A correlation between the applied compaction force and the acoustic signal was found. Also the phenomenon of lamination, which regularly occurs during roll compaction, influenced the signal and could be monitored. It has been criticized by these authors and others that the signal to noise ratio of this approach was insufficient [65]. It is furthermore not clear, if the acoustic emissions really correlate to the densification of the powder (i.e. solid fraction), or just to the applied force. This is relevant, because it is well described that also other process parameters like the gap width affect the ribbon solid fraction. A reliable PAT tool should give a signal that really depends on the solid fraction, and does not just correlate with the applied force. Without thorough testing of the robustness towards changes of different process parameters, an evaluation of the applicability of a PAT tool is not possible.

Another technique that has been used is microwave resonance sensing. In a comparison study with NIR spectroscopy, it gave slightly more accurate predictions of ribbon density [66]. The sensor that was used in the study was however too large to fit into the production chamber of a roll compactor. The ribbon was guided by a conveyor belt to the sensor that was installed outside the machine. This is not appropriate for pharmaceutical manufacturing, especially if highly potent APIs are used. Furthermore, such a conveying system only works if a continuous and intact ribbon is produced, which might be the case for pure microcrystalline cellulose (as was used in the study), but not for a wide range of other materials. This technique is hence not suitable to be applied in an industrial environment in its current form.

The most used PAT tool in the field of RCDG is NIR spectroscopy [65]. A first series of studies was performed by Gupta et al. In the first study, an upward shift of the absorption

spectra with increasing compaction pressure was observed [67]. This shift was more pronounced at higher wavelengths, so that the slope of the best-fit line could be used as a response and be correlated to the breaking force as a surrogate for the solid fraction as well as to the median particle size. In a subsequent study, partial least squares (PLS) models were constructed based on off-line NIR measurements and used to make real-time predictions [68]. The predictions were systematically biased, which the authors hypothesized to be the result of slow elastic recovery that has occurred in the ribbons used for off-line calibration. The authors concluded that calibration data should be obtained under conditions as close as possible to the actual experiments. When characterization was performed immediately after production, the predictions showed better alignment with reference values [69]. In that study, PLS models were successfully used to predict moisture, tensile strength, solid fraction, Young's Modulus, and API concentration. It was however not investigated to what extent these factors can be monitored separately. Regarding solid fraction, tensile strength, and Young's Modulus, it is questionable if a separate contemplation is even reasonable, since all these measures are strongly linked. Avecedo et al. published a study comparing the suitability of different calibration models for NIR spectroscopy in roll compaction [32]. They concluded that principle component analysis (PCA) is the most reliable approach to monitor roll compaction. Since PCA does not link the spectra to reference data, it is only able to give qualitative information. In this context, this means changes in the product are detected, but no prediction regarding the extent or the relevance of the change can be made. If this approach is really sufficient to control the quality of pharmaceutical products is questionable. Khorasani et al. used NIR chemical imaging to monitor not only the overall ribbon solid fraction, but also the distribution within the ribbon [36, 37]. Also in these studies, a correlation of the NIR signal was demonstrated not only with the ribbon solid fraction, but also with the GSD.

General disadvantages of NIR spectroscopy as a PAT tool for RCDG are a high noise in spectra, a high dependence to the exact way in which the ribbon is presented to the probe, and systematic biases due to slow elastic recovery [65, 70]. As already described for microwave resonance sensing, the NIR probe was placed outside of the roll compactor in all studies for which the set-up was described in detail and hence also hardly applicable in pharmaceutical manufacturing in its current form. Furthermore, these studies have been performed on lab scale roll compactors with a static gap and without automatic gap control. With these roll compactors, the possibility to study the robustness of the measuring

technique towards changes in process parameters is limited. It is for example not possible to test the robustness of the NIR signal towards changes in gap width. Such studies however are necessary to evaluate the suitability of a PAT tool for a certain process. Moreover, PAT tools are especially important to detect changes in the process, that cannot be observed by monitoring the process parameters. Such changes can be caused i.a. by inter-batch variations of excipients or changes in the climatic conditions. So far no published study was conducted that critically tested, if a PAT tool has any benefit to monitoring the process parameters during roll compaction.

Several studies have linked NIR spectra of ribbons to GSD after subsequent milling, a direct measurement of GSD is however advisable. The reason for this is that even though ribbon solid fraction strongly affects GSD after milling, it is not the only parameter influencing GSD [30]. The literature regarding this subject is limited. One approach is granule size measurement by the fiber-optic spatial filter method [71]. The in-line results differed significantly from reference measurements, probably because it was not possible to continuously guide a representative fraction of the granules to the probe.

## **1.2 X-ray micro-computed tomography**

### **1.2.1 General**

X-ray micro-computed tomography ( $X\mu$ CT) is a non-destructive three-dimensional imaging technique [72, 73]. A conical X-ray beam is used to project a sample onto a suitable detector to obtain X-ray images. In contrast to two-dimensional X-ray imaging, such projections are obtained from multiple angles and the data is subsequently reconstructed to a three-dimensional image.

Computer tomographs mainly consist of three functional units: an X-ray source, a sample holder, and a detector. In conventional set-ups, which are mainly used in medical research and diagnostics, the sample (= body) is static while the X-ray source and detector rotate around it. For  $X\mu$ CT however, the X-ray tube and detector are static while the sample rotates (see Figure 1-4). In such a set-up, the X-ray beam follows a conical shape, which results in a magnified projection on the detector. Hence, the magnification can be varied by the position of the sample between tube and detector. The closer to the tube a sample is placed, the higher is the achieved magnification. The resolution of the acquired image depends on the number of pixels on the detector. The voxel size, which is usually given in literature, depends on the detector pixel size as well as on the ratio of sample-detector and

focus-sample distance. Voxel sizes down to approximately  $0.4 \mu\text{m}$  can be achieved in commercially available systems.

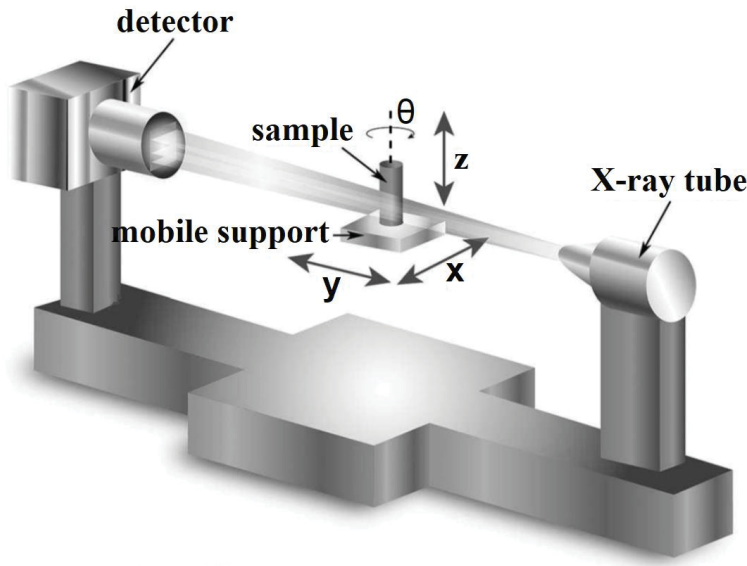


Figure 1-4: Set-up of 3D X-ray micro-computed tomography, modified from Gómez et al.[74]

While passing through the sample, the X-ray radiation is partially absorbed and the decrease in radiation energy is captured by the detector pixels. The absorption behavior of X-rays in a given material was described by McCullough [75] (see eq. 2).

$$\mu = \rho \frac{Z}{A} N_{AV} \left( a + b \frac{Z^{3.8}}{E^{3.2}} \right) \quad (2)$$

The attenuation coefficient ( $\mu$ ) depends on the material density ( $\rho$ ), the effective atomic number ( $Z$ ), the atomic mass ( $A$ ), and the photon energy ( $E$ ).  $N_{AV}$  is Avogadro's number, (a) the Klein-Nishina-coefficient, and (b) a further dimensionless constant. From this follows that materials can be distinguished in a X $\mu$ CT image if they are either composed of different elements or are of different density (or both).

X $\mu$ CT imaging is prone to a variety of different artifacts which are caused by number of physical phenomena. So called *ring artifacts* are common and a challenge for image segmentation [76]. They are caused by the fact that not all detector pixels show the same sensitivity to radiation, i.e. the same radiation does not result in the same gray value on every pixel. The rotation of the sample during measurement leads to circular lines of deviating grey value in the reconstructed image. These artifacts can be reduced by certain arrangements of the set-up as well as by sophisticated algorithms during reconstruction [76]. Another type of artifact that can be of high relevance is caused by beam hardening

(hence called *beam hardening artifacts*) [77]. Even though a precise acceleration voltage (e.g. 100 kV) can be applied in the X-ray tube, the resulting electromagnetic radiation is not monochromatic. It does not only show photon energies that correspond to the applied voltage (in this example 100 keV), but also a broad spectrum of lower photon energies. As demonstrated in Eq. 2, the absorption by the sample also depends on the radiation energy, so that while passing through the sample not only the absolute energy is changed, but also the radiation spectrum. Regions in the center of the sample are hence exposed to radiation of a different spectrum. Consequently, they will show a different (lower) absorption than a region of identical composition and density that is located near the surface. This phenomenon is well described for highly absorbing materials like metals or bones and usually deemed negligible for organic materials [78]. If however density distributions within samples are to be quantified, this effect might significantly affect the results. The possibilities to compensate beam hardening artifacts mathematically during reconstruction are limited, but the artifacts can be reduced by installation of filters between X-ray tube and sample [79]. These filters consist of highly absorbing materials (e.g. copper) and narrow the radiation spectrum by predominantly absorbing softer radiation.

### 1.2.2 Pharmaceutical applications

The use of X $\mu$ CT is relatively new to pharmaceutical research, the first study using this technique was published in 2003 [45, 80]. In the last 15 years however, it has become widely accepted and has been applied on a wide range of subjects. Even though the applications are diverse, most of them can be summarized in a few groups. In a great number of studies, X $\mu$ CT has been used to determine the outer geometry, volume, or surface area of dosage forms or intermediate products [81-85]. Especially in the field of personalized medicine, dosage forms of a high diversity are produced for which standard analytical characterization is not feasible. In several studies, solid dosage forms have been produced by 3D printing and subsequently analyzed by X $\mu$ CT [81-83, 85, 86]. Korte and Quodbach used surface areas determined by X $\mu$ CT to predict drug release profiles of 3D printed network structures [87]. This study could also be seen as part of a second group of applications, in which matrix structures for sustained release are scanned by X $\mu$ CT and either the pore structure or API distribution was determined and linked to respective dissolution profiles [84, 88-90]. In a number of studies, also structural changes in the matrix during dissolution have been visualized. An increase in number and size of pores could

gradually be detected for tablets which were taken and dried at various points during dissolution [81, 88].

X $\mu$ CT is well suited to measure the coating thickness on tablets [91, 92] and pellets [93]. If functional coatings are used, the coating thickness is a critical quality attribute with potentially drastic impact on drug safety and efficacy. Hence, a lot of effort is put into developing a suitable PAT tool. X $\mu$ CT is not a candidate for this for a number of reasons, for example the long measuring times and the large dimension. It has however been used as a reference method for validation of potential PAT tools like Terahertz spectroscopy [91], NIR spectroscopy [92], and optical coherence tomography [93]. A very ambitious aim for which X $\mu$ CT has been used is to gain mechanistic understanding of physical properties by identification and studying of primary particles within solid dosage forms. It is challenging, because most excipients are organic and hence differences in elementary constitution and density are limited. Thus, the contrast in X $\mu$ CT is low and a reliable differentiation between materials therefore difficult [80]. A series of studies has been published by a Chinese research group who used a synchrotron X-ray tomography set-up. Using synchrotrons as a source of X-ray radiation has the advantage that the energy is orders of magnitudes higher than in conventional X-ray tubes, leading to higher contrasts. Furthermore, the radiation is monochromatic which eliminates the cause of artifacts and the radiation is by nature highly focused [94, 95]. With synchrotron X-ray tomography, it was possible to investigate the mechanism of taste-masking in microspheres [96] and to correlate structural differences of MCC particles of the same grade but from different suppliers to their binding ability [97]. Unfortunately, synchrotron set-ups are rare, the measurements are expensive, and access usually limited. Despite the high potential of this technique to give valuable information in the structural properties of solid dosage forms, it is unlikely to become a standard method.

Probably the largest group of applications for X $\mu$ CT in pharmaceutical technology are pore system analyses. As laid out in section 1.1.2, pores can be identified by binarization of the original gray scale image. Zeitler et. al stated that pore size analysis by X $\mu$ CT has the great advantage over mercury porosimetry to reveal the actual pore size instead of “neck” diameters and to give additional information on shape and connectivity of pores [80]. The disadvantage however is that the sensitivity to small pores is limited by the voxel size, while mercury porosimetry allows determination of pore sizes in the low nanometer range [45, 80]. If not the pore size distribution but only the porosity/solid fraction is of

interest, oftentimes scans of low resolution are performed and the resulting gray value of a discrete region taken as a marker (as laid out in section 1.1.2). Using this approach, the solid fraction in tablets as well as in ribbons has been investigated. A number of studies concordantly found characteristic distribution patterns, depending on the tablet shape [98, 99].

### 1.3 Infrared thermography

#### 1.3.1 General

Infrared radiation is electromagnetic radiation of wavelengths between 780 nm and 1 mm [100, 101]. It is emitted from every object whose temperature is higher than 0 K [101, 102]. As described by the Stefan-Boltzmann equation (Eq. 3), the power of emitted radiation ( $P$ ) per surface area ( $A$ ) depends on the surface temperature  $T$  and the Stefan-Boltzmann constant  $\sigma$  [103].

$$\frac{P}{A} = T^4 * \sigma \quad (3)$$

The emitted radiation is not monochromatic, but shows a broad range of wavelengths, as is displayed in Figure 1-5. Following Wien's displacement law, the radiation is shifted to shorter wavelengths with higher temperatures [104]. At temperatures above about 1000 K, radiation within the visible range is emitted, which can be captured by the human eye ("glowing"). At the more moderate temperatures which occur during pharmaceutical processing, the radiation is solely in the infrared range. Due to the dependence of intensity and wavelength from the surface temperature, the surface temperature can be derived from the infrared radiation. Usually, radiation of a limited bandwidth is considered for this and the temperature derived solely from the radiation energy. For most applications, the bandwidth between 7.5 and 13  $\mu\text{m}$  is used [101, 105]. This bandwidth is used on the one hand because a wide range of temperatures induce radiation in this bandwidth. On the other hand, air is not transparent for most wavelengths of the infrared range [106]. Water/steam contained in the air shows absorption at wavelengths below 7-8  $\mu\text{m}$ , while carbon dioxide absorbs at wavelengths above ca. 15  $\mu\text{m}$ , leaving the range between 7.5 and 13  $\mu\text{m}$  for unrestricted measurements ("atmospheric window").

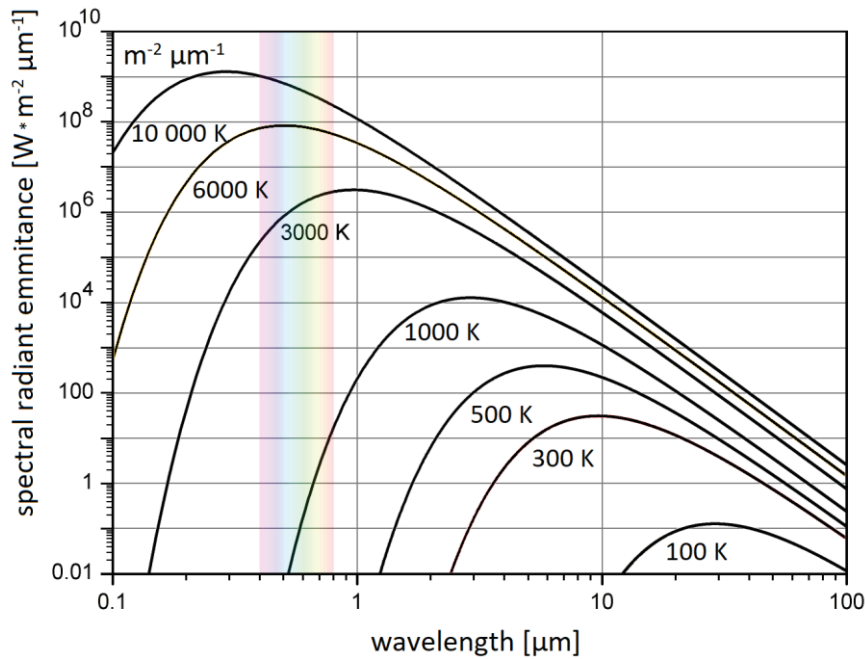


Figure 1-5: emission spectra of black bodies at various temperatures, modified from Stricker[107]

Thermographic cameras are set-up equivalently to conventional digital cameras, but use different materials for lenses and detection units. Since glass is not transparent for infrared radiation, lenses for infrared thermography are usually made from sodium chloride or germanium [108]. This lens focuses the incoming radiation onto a detector, which is in modern infrared cameras a microbolometer array [108]. Each element of this array is build up from an absorbing membrane, an infrared mirror, a semiconductive sensor layer, and two electrodes (see Figure 1-6). If exposed to infrared radiation, the membrane heats up and the heat is conducted to the sensor layer, which changes its electric conductivity. The efficiency is increased by a mirror, which reflects portions of radiation that could not be absorbed back on the membrane. With heating of the semiconductive layer, the current between the electrodes increases and can be detected. The sensor layer can be made of vanadium oxide or amorphous silicon. Since the pixels of bolometric arrays are about tenfold larger than the charge-coupled devices (CCD) used in digital cameras for the optical range ( $17$  vs.  $1.4 \mu\text{m}$ ), the resolution of thermographic cameras is limited [109]. Commercially available cameras typically allow resolutions of up to  $640 \times 480$  pixels.

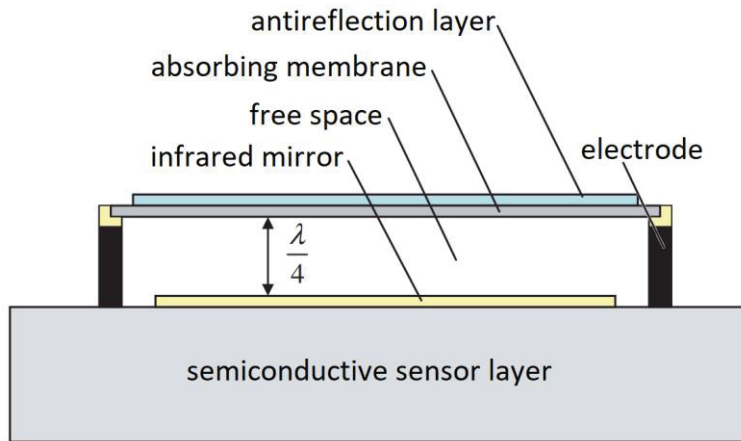


Figure 1-6: schematic set-up of bolometer detector, modified from Niklaus et al. [111]

To derive the object temperature from infrared radiation, it has to be considered that the samples are not ideal black bodies, i.e. not all infrared radiation leaving the object does not originate from emission ( $\epsilon$ ) only. Parts of it also originate from reflection ( $\rho$ ) and/or transmission ( $\tau$ ) (see Eq. 4) [102].

$$\epsilon + \rho + \tau = 1 \quad (4)$$

To accurately determine the surface temperature, the emissivity of the material has to be taken into account. Most materials have an emissivity of about 0.9, but some highly reflecting materials (especially metals) have emissivity values down to 0.2-0.3 [108]. If not properly respected, this will lead to severely biased measuring results. Precise knowledge of the emissivity is especially important, if objects of different composition are compared. If objects of the same material are to be compared, and only relative differences are of interest, also the assumption of an ideal black body ( $\epsilon = 1$ ) might be acceptable [108]. The absolute values will be biased, but measurements of relative differences and trends are still valid.

### 1.3.2 Pharmaceutical applications

The use of thermographic imaging in pharmaceutical technology is not new, but the number of published studies has massively increased in the last decade. The applications are diverse and focus mainly on the thermal stress during compaction [111-115] or drying [116]. The first study was published in 1992 and focused on the temperature rise during tablet compression [111]. A dependency of the tablet temperature after compression from the applied compression force was found. Higher concentrations of magnesium stearate decreased the temperatures. This effect became more pronounced over process time.

Interestingly, the highest thermal stress was observed not at the top where the compression force is conveyed, but at the tablet edges where the wall-die friction occurs. A series of studies was published by Zavaliangos et al., who used thermography to validate finite element models on thermal stress during tablet compression [113-115]. In addition to previous knowledge, they also observed an effect of compression speed on tablet temperature. Also a certain agreement of temperature distribution and densification level could be observed. Similar experiments with confirming results were conducted by Krok et al. [112]. The same authors also used thermography to test common models describing thermal conductivity of porous solids in dependency from their solid fraction [117]. The two models describing this dependency were proposed by Maxwell [118, 119] and Zavaliangos [114]. Both models predict a steady increase of thermal conductivity with higher solid fractions.

Omar et. al applied a thermographic camera to a lab scale roll compactor to study the effect of particle morphology on inter-particulate friction during compaction [42]. A second study by the same group found that ribbon temperature predominantly depends on the gap width during production and compaction force had a secondary effect [43]. In a recent study aiming at improved homogeneity of solid fraction in ribbons, they used thermography to visualize temperature patterns [41]. The validity of temperature distribution as a surrogate for solid fraction distribution was tested by cutting the ribbons in five pieces and determining the respective solid fraction.

### **1.4 Aims of the thesis**

As laid out in the previous sections, a reliable PAT tool for monitoring the ribbon solid fraction during RCDG is highly desired. This tool should be able to predict solid fractions accurately and precisely, while being robust to changes in process parameters, climatic conditions, and process time. It should further be applicable to commercially available roll compactors without the need to artificially convey to an analytical set-up placed outside the roll compactor. A reasonable application in pharmaceutical manufacturing would only be possible if the sensor is small enough to fit into the production chamber. Furthermore, the analytical tool should be applicable on a wide range of materials. Most PAT tools that are already established in pharmaceutical industry are highly expensive and require an extensive chemometric analysis. An ideal PAT tool however should be relatively inexpensive and give reliable results without the need for complex modelling.

In detail, the aims of this thesis were as follows:

- To investigate the principal potential of infrared thermography to monitor ribbon solid fraction during roll compaction. A technical set-up as well as suitable data analysis procedure should be developed and markers should be defined.
- To test the robustness of this new technique towards process parameters, process time, climatic conditions, and material properties. Based on the results, the potentials and limitations for its applicability in pharmaceutical manufacturing should be estimated.
- To use X $\mu$ CT measurements to visualize and analyze the distribution of solid fraction within ribbons. A complete understanding of distribution patterns in dependence of the sealing system should be achieved.
- To answer if and how process parameters can be used to affect ribbon homogeneity.
- To use X $\mu$ CT measurements to critically evaluate the relevance of ribbon homogeneity for subsequent processing. Particularly the influence on strength and mass variability of tablets compressed from dry granules should be investigated. Based on the findings, the relevance of monitoring ribbon homogeneity in-line should be estimated.
- To analyze the possibility to determine ribbon solid fraction based on the thermal conductivity. A device should be designed that allows the artificial input of thermal energy into the ribbon, an analytical method established, and reasonable markers defined. A suitable way of data processing and data analysis should be compiled.
- To test, if the developed method gives information on the ribbon quality that goes beyond information that can be drawn from monitoring the process parameters.

### 1.5 Outline of the thesis

The underlying work of this thesis can be divided into two main parts, each consisting of several sub-sections. In the first main part, the ribbon homogeneity was investigated thoroughly. To do so, the solid fraction distribution within ribbons was analyzed by X $\mu$ CT and focused especially on details that have not been described in literature, yet. That is the distribution over ribbon thickness for ribbons produced with both sealing systems, cheek plates as well as rim rolls, and the distribution along ribbon length for rim rolls ribbons. Based on that, a full description of the ribbon homogeneity in all three spatial directions was accessed. By periodicity analysis, also existing hypotheses on the cause of certain patterns could be confirmed. In the second sub-section of this part, it was investigated, if

and how process parameters can be used to affect the homogeneity of ribbons. It was furthermore studied, how relevant this homogeneity is for subsequent processing. Tablet compression was selected as the most important subsequent process and tablet strength and tablet mass variability were used as markers. Based on the results, it was evaluated, if it is reasonable and necessary to monitor ribbon homogeneity during RCDG processes.

The second main part was the testing of infrared thermography as a technique to monitor ribbon solid fraction in-line. In a first step, the principle ability of the approach was studied. The focus was on correlation of ribbon temperature and solid fraction, for the entire ribbon as well as spatially resolved. To already allow first estimations on the applicability, the reaction time to changes in process parameters was measured. Furthermore, another thermal characteristic, namely the cooling rate after compaction, was analyzed and an estimation made if this marker is suitable for in-line determination of ribbon solid fraction. In the following sub-section, the practical applicability of thermography as an in-line measuring tool during RCDG was critically tested. The focus was especially on the range of materials, including lubricants and glidants, on which the technique can be applied. Also the robustness towards changes in climatic conditions, changes in process parameters, and long process times was tested. Finally, the predictive potential was critically evaluated. Based on the results of this applicability study, a new in-line measuring device was constructed and tested. It also uses thermography, but is based on a different physical principle: the dependence of thermal conductivity from solid fraction. Suitable markers regarding sensitivity and robustness were defined and the influence of the energy input on the product quality tested using nifedipine as a model drug.

## References

- [1] E.L. Parrott, Densification of powders by concavo-convex roller compactor, *J. Pharm. Sci.*, 70 (1981) 288-291.
- [2] R.W. Miller, Advances in pharmaceutical roller compactor feed system designs, *Pharm. Technol. Eur.*, 6 (1994) 58-68.
- [3] P. Kleinebudde, Roll compaction/dry granulation: pharmaceutical applications, *Eur. J. Pharm. Biopharm.*, 58 (2004) 317-326.
- [4] J. Mosig, Untersuchung des Tablettierverhaltens von Trockengranulaten verschiedener Hilfsstoffe, PhD Thesis, Heinrich Heine University, Düsseldorf, 2014.
- [5] P. Guigon, O. Simon, Roll press design - Influence of force feed systems on compaction, *Powder Technol.*, 130 (2003) 41-48.
- [6] A. Mazor, L. Perez-Gandarillas, A. de Ryck, A. Michrafy, Effect of roll compactor sealing system designs: A finite element analysis, *Powder Technol.*, 289 (2016) 21-30.
- [7] A. Fahr, X. Liu, Drug delivery strategies for poorly water-soluble drugs, *Expert Opinion on Drug Delivery*, 4 (2007) 403-416.
- [8] S. Malkowska, K.A. Khan, Effect of re-compression on the properties of tablets prepared by dry granulation, *Drug Dev. Ind. Pharm.*, 9 (1983) 331-347.
- [9] C. Sun, M.W. Himmelpach, Reduced tableability of roller compacted granules as a result of granule size enlargement, *J. Pharm. Sci.*, 95 (2006) 200-206.
- [10] M.G. Herting, P. Kleinebudde, Letter to the editor, *Int. J. Pharm.*, 347 (2008) 173-174.
- [11] M.G. Herting, P. Kleinebudde, Roll compaction/dry granulation: Effect of raw material particle size on granule and tablet properties, *Int. J. Pharm.*, 338 (2007) 110-118.
- [12] J. Mosig, P. Kleinebudde, Critical evaluation of root causes of the reduced compactability after roll compaction/dry granulation, *J. Pharm. Sci.*, 104 (2015) 1108-1118.
- [13] C.C. Sun, P. Kleinebudde, Mini review: Mechanisms to the loss of tableability by dry granulation, *Eur. J. Pharm. Biopharm.* 106 (2016) 9-14.
- [14] M. Leane, K. Pitt, G. Reynolds, J. Anwar, S. Charlton, A. Crean, R. Creekmore, C. Davies, T. DeBeer, M. De-Matas, A. Djemai, D. Douroumis, S. Gaisford, J. Gamble, E.H. Stone, A. Kavanagh, Y. Khimyak, P. Kleinebudde, C. Moreton, A. Paudel, R. Storey, G. Toschkoff, K. Vyas, A proposal for a drug product Manufacturing Classification System (MCS) for oral solid dosage forms, *Pharm. Dev. Technol.*, 20 (2015) 12-21.
- [15] *Continuous Manufacturing of Pharmaceuticals*, P. Kleinebudde, J. Khinast, J. Rantanen, Wiley, 2017.
- [16] H. Leuenberger, New trends in the production of pharmaceutical granules: Batch versus continuous processing, *Eur. J. Pharm. Biopharm.*, 52 (2001) 289-296.
- [17] J. Rantanen, J. Khinast, The future of pharmaceutical manufacturing sciences, *J. Pharm. Sci.*, 104 (2015) 3612-3638.
- [18] C. Vervaet, J.P. Remon, Continuous granulation in the pharmaceutical industry, *Chem. Eng. Sci.*, 60 (2005) 3949-3957.

- [19] J.R. Johanson, A rolling theory for granular solids, *J Appl Mech Trans ASME*, 32 (1964) 842-848.
- [20] S. Peter, R.F. Lammens, K.-J. Steffens, Roller compaction/Dry granulation: Use of the thin layer model for predicting densities and forces during roller compaction, *Powder Technol.*, 199 (2010) 165-175.
- [21] J.C. Cunningham, D. Winstead, A. Zavaliangos, Understanding variation in roller compaction through finite element-based process modeling, *Comput. Chem. Eng.*, 34 (2010) 1058-1071.
- [22] R.F. Mansa, R.H. Bridson, R.W. Greenwood, H. Barker, J.P.K. Seville, Using intelligent software to predict the effects of formulation and processing parameters on roller compaction, *Powder Technol.*, 181 (2008) 217-225.
- [23] S. Inghelbrecht, J.P. Remon, P. Fernandes De Aguiar, B. Walczak, D.L. Massart, F. Van De Velde, P. De Baets, H. Vermeersch, P. De Backer, Instrumentation of a roll compactor and the evaluation of the parameter settings by neural networks, *Int. J. Pharm.*, 148 (1997) 103-115.
- [24] R. Fassihi, I. Kanfer, Effect of Compressibility and Powder Flow Properties on Tablet Weight Variation, *Drug Dev. Ind. Pharm.*, 12 (1986) 1947-1966.
- [25] S.B. Tan, J.M. Newton, Powder flowability as an indication of capsule filling performance, *Int. J. Pharm.*, 61 (1990) 145-155.
- [26] M. Wikberg, G. Alderborn, Compression characteristics of granulated materials. IV. The effect of granule porosity on the fragmentation propensity and the compatibility of some granulations, *Int. J. Pharm.*, 69 (1991) 239-253.
- [27] M.A. Ansari, F. Stepanek, The effect of granule microstructure on dissolution rate, *Powder Technol.*, 181 (2008) 104-114.
- [28] J. Nordström, G. Alderborn, The granule porosity controls the loss of compactibility for both dry- and wet-processed cellulose granules but at different rate, *J. Pharm. Sci.*, 104 (2015) 2029-2039.
- [29] F. Jaminet, H. Hess, Studies on compacting and dry granulation, *Pharm. Acta Helv.*, 41 (1966) 39-58.
- [30] H. Mangal, P. Kleinebudde, Is the adjustment of the impeller speed a reliable attempt to influence granule size in continuous dry granulation?, *Adv. Powder Technol.*, 29 (2018) 1339-1347.
- [31] R. Ramachandran, J.M.H. Poon, C.F.W. Sanders, T. Glaser, C.D. Immanuel, F.J. Doyle, J.D. Litster, F. Stepanek, F.-Y. Wang, I.T. Cameron, Experimental studies on distributions of granule size, binder content and porosity in batch drum granulation: Inferences on process modelling requirements and process sensitivities, *Powder Technol.*, 188 (2008) 89-101.
- [32] D. Acevedo, A. Muliadi, A. Giridhar, J.D. Litster, R.J. Romañach, Evaluation of three approaches for real-time monitoring of roller compaction with near-infrared spectroscopy, *AAPS PharmSciTech*, 13 (2012) 1005-1012.
- [33] A.K. Samanta, A.D. Karande, K.Y. Ng, P.W.S. Heng, Application of near-infrared spectroscopy in real-time monitoring of product attributes of ribbed roller compacted flakes, *AAPS PharmSciTech*, 14 (2013) 86-100.

- [34] A. Michrafy, H. Diarra, J.A. Dodds, M. Michrafy, Experimental and numerical analyses of homogeneity over strip width in roll compaction, *Powder Technol.*, 206 (2011) 154-160.
- [35] G. Alderborn, E. Borjesson, M. Glazer, C. Nystrom, Studies on direct compression of tablets. XIX. The effect of particle size and shape on the mechanical strength of sodium bicarbonate tablets, *Acta Pharm. Suecica*, 25 (1988) 31-40.
- [36] M. Khorasani, J.M. Amigo, C.C. Sun, P. Bertelsen, J. Rantanen, Near-infrared chemical imaging (NIR-CI) as a process monitoring solution for a production line of roll compaction and tableting, *Eur. J. Pharm. Biopharm.*, 93 (2015) 293-302.
- [37] M. Khorasani, J.M. Amigo, P. Bertelsen, C.C. Sun, J. Rantanen, Process optimization of dry granulation based tableting line: Extracting physical material characteristics from granules, ribbons and tablets using near-IR (NIR) spectroscopic measurement, *Powder Technol.*, 300 (2016) 120-125.
- [38] M. Allesø, R. Holm, P. Holm, Roller compaction scale-up using roll width as scale factor and laser-based determined ribbon porosity as critical material attribute, *Eur. J. Pharm. Sci.*, 87 (2016) 69-78.
- [39] R.M. Iyer, S. Hegde, D. Singhal, W. Malick, A novel approach to determine solid fraction using a laser-based direct volume measurement device, *Pharm. Dev. Technol.*, 19 (2014) 577-582.
- [40] C. Solid Fraction Measurement Systems, CT, USA, Laser-Based Solid Fraction Measurement System- System Overview, in, *Solid Fraction Measurement Systems*, Centerbrook, CT, USA, [http://solidfraction.com/solid\\_fraction\\_measurements.html](http://solidfraction.com/solid_fraction_measurements.html).
- [41] M. Yu, C. Omar, A. Schmidt, J.D. Litster, A.D. Salman, Improving feeding powder distribution to the compaction zone in the roller compaction, *Eur. J. Pharm. Biopharm.*, 128 (2018) 57-68.
- [42] C.S. Omar, R.M. Dhenge, J.D. Osborne, T.O. Althaus, S. Palzer, M.J. Hounslow, A.D. Salman, Roller compaction: Effect of morphology and amorphous content of lactose powder on product quality, *International Journal of Pharmaceutics*, 496 (2015) 63-74.
- [43] R.B. Al-Asady, R.M. Dhenge, M.J. Hounslow, A.D. Salman, Roller compactor: Determining the nip angle and powder compaction progress by indentation of the pre-compacted body, *Powder Technol.*, 300 (2016) 107-119.
- [44] S.R. Stock, X-ray microtomography of materials, *Int. Mater. Rev.*, 44 (1999) 141-164.
- [45] L. Farber, G. Tardos, J.N. Michaels, Use of X-ray tomography to study the porosity and morphology of granules, *Powder Technol.*, 132 (2003) 57-63.
- [46] A.M. Miguélez-Morán, C.Y. Wu, H. Dong, J.P.K. Seville, Characterisation of density distributions in roller-compacted ribbons using micro-indentation and X-ray micro-computed tomography, *Eur. J. Pharm. Biopharm.*, 72 (2009) 173-182.
- [47] N. Souihi, D. Nilsson, M. Josefson, J. Trygg, Near-infrared chemical imaging (NIR-CI) on roll compacted ribbons and tablets - Multivariate mapping of physical and chemical properties, *Int. J. Pharm.*, 483 (2015) 200-211.
- [48] F. Wöll, P. Kleinebudde, Characterization of the porosity of compacted powders: stamping method and NIRS method, *Chem. Ing. Tech.*, 75 (2003) 1756-1759+1581.

- [49] J.D. Kirsch, J.K. Drennen, Nondestructive tablet hardness testing by near-infrared spectroscopy: A new and robust spectral best-fit algorithm, *J. Pharm. Biomed. Anal.*, 19 (1999) 351-362.
- [50] D. Markl, P. Wang, C. Ridgway, A.P. Karttunen, M. Chakraborty, P. Bawuah, P. Pääkkönen, P. Gane, J. Ketolainen, K.E. Peiponen, J.A. Zeitler, Characterization of the pore structure of functionalized calcium carbonate tablets by terahertz time-domain spectroscopy and X-ray computed microtomography, *J. Pharm. Sci.*, 106 (2017) 1586-1595.
- [51] Y. Funakoshi, T. Asogawa, E. Satake, The use of a novel roller compactor with a concavo-convex roller pair to obtain uniform compacting pressure, *Drug Dev. Ind. Pharm.*, 3 (1977) 555-573.
- [52] I. Akseli, S. Iyer, H.P. Lee, A.M. Cuitiño, A quantitative correlation of the effect of density distributions in roller-compacted ribbons on the mechanical properties of tablets using ultrasonics and X-ray tomography, *AAPS PharmSciTech*, 12 (2011) 834-853.
- [53] O. Simon, P. Guigon, Interaction between feeding and compaction during lactose compaction in a laboratory roll press, *KONA Powder Part. J.*, 18 (2000) 131-138.
- [54] F. Wöll, Entwicklung von Methoden zur Charakterisierung von Schülpen, PhD thesis, Martin-Luther-Universität Halle-Wittenberg, Halle a.d. Saale, 2003.
- [55] H. Busies, Dichteverteilung in Schülpen, PhD thesis, Universität Bonn, 2006.
- [56] S. Peter, R.F. Lammens, K.-J. Steffens, Roller Compaction: Improving homogeneity of ribbon density by modifying powder supply, *Tablet Tech Seminar*, FMC Biopolymer, Brussels, Belgium, 2007.
- [57] A.M. Miguélez-Morán, C.Y. Wu, J.P.K. Seville, The effect of lubrication on density distributions of roller compacted ribbons, *Int. J. Pharm.*, 362 (2008) 52-59.
- [58] W.A. Strickland Jr, E. Nelson, L.W. Busse, T. Higuchi, The physics of tablet compression. IX. Fundamental aspects of tablet lubrication, *J. Am. Pharm. Assoc. Sci.*, 45 (1956) 51-55.
- [59] G.K. Bolhuis, A.J. Smallenbroek, C.F. Lerk, Interaction of tablet disintegrants and magnesium stearate during mixing I: Effect on tablet disintegration, *J. Pharm. Sci.*, 70 (1981) 1328-1330.
- [60] *Prozessanalytik: Strategien und Fallbeispiele aus der industriellen Praxis*, Rudolf W. Kessler, Wiley, 2006.
- [61] *Guidance for Industry PAT — A framework for innovative pharmaceutical development, manufacturing, and quality assurance*, U.S. Food and Drug Administration, Silver Spring, MD, USA, 2004.
- [62] R. Luigetti, QbD: A global implementation perspective - The EU perspective, *The Siena Conference on Product and Process Optimization*, EMA, Siena, 2008.
- [63] A. Hakanen, E. Laine, Acoustic emission during powder compaction and its frequency spectral analysis, *Drug Development and Industrial Pharmacy*, 19 (1993) 2539-2560.
- [64] A. Hakanen, E. Laine, Acoustic characterization of a microcrystalline cellulose powder during and after its compression, *Drug Development and Industrial Pharmacy*, 21 (1995) 1573-1582.

- [65] M. Fonteyne, J. Vercruyse, F. De Leersnyder, B. Van Snick, C. Vervaet, J.P. Remon, T. De Beer, Process Analytical Technology for continuous manufacturing of solid-dosage forms, *TrAC Trends Anal. Chem.*, 67 (2015) 159-166.
- [66] J. Austin, A. Gupta, R. McDonnell, G.V. Reklaitis, M.T. Harris, The use of near-infrared and microwave resonance sensing to monitor a continuous roller compaction process, *J. Pharm. Sci.*, 102 (2013) 1895-1904.
- [67] A. Gupta, G.E. Peck, R.W. Miller, K.R. Morris, Nondestructive measurements of the compact strength and the particle-size distribution after milling of roller compacted powders by near-infrared spectroscopy, *J. Pharm. Sci.*, 93 (2004) 1047-1053.
- [68] A. Gupta, G.E. Peck, R.W. Miller, K.R. Morris, Influence of ambient moisture on the compaction behavior of microcrystalline cellulose powder undergoing uni-axial compression and roller-compaction: A comparative study using near-infrared spectroscopy, *J. Pharm. Sci.*, 94 (2005) 2301-2313.
- [69] A. Gupta, G.E. Peck, R.W. Miller, K.R. Morris, Real-time near-infrared monitoring of content uniformity, moisture content, compact density/tensile strength, and young's modulus of roller compacted powder blends, *J. Pharm. Sci.*, 94 (2005) 1589-1597.
- [70] M.E. Crowley, A. Hegarty, M.A.P. McAuliffe, G.E. O'Mahony, L. Kiernan, K. Hayes, A.M. Crean, Near-infrared monitoring of roller compacted ribbon density: Investigating sources of variation contributing to noisy spectral data, *Eur. J. Pharm. Sci.*, 102 (2017) 103-114.
- [71] H. Mangal, Implementierung der Trockengranulierung in eine kontinuierliche Produktionsanlage für feste Arzneiformen, PhD thesis, Heinrich Heine University, Düsseldorf, 2018.
- [72] J.C. Elliott, S.D. Dover, X-ray microtomography, *J. Microsc.*, 126 (1982) 211-213.
- [73] R. Wiedey, P. Kleinebudde, Density distribution in ribbons from roll compaction, *Chem Ing Tech*, 89 (2016) 1017-1024.
- [74] W. Gómez, E. Sales, R.T. Lopes, W.C.A. Pereira, A comparative study of automatic thresholding approaches for 3D X-ray microtomography of trabecular bone, *Med. Phys.*, 40 (2013) Article number 091903.
- [75] E.C. McCullough, Photon attenuation in computed tomography, *Med. Phys.*, 2 (1975) 307-320.
- [76] G. Kowalski, Suppression of ring artefacts in ct fan-beam scanners, *IEEE Trans Nucl Sci*, 25 (1978) 1111-1116.
- [77] R.A. Brooks, G. Di Chiro, Beam hardening in X-ray reconstructive tomography, *Phys. Med. Biol.*, 21 (1976) 390-398.
- [78] P. Sridhar Rao, R.J. Alfidi, The environmental density artifact: A beam-hardening effect in computed tomography, *Radiology*, 141 (1981) 223-227.
- [79] P.K. Kijewski, B.E. Bjärngard, Correction for beam hardening in computed tomography, *Med. Phys.*, 5 (1978) 209-214.
- [80] J.A. Zeitler, L.F. Gladden, In-vitro tomography and non-destructive imaging at depth of pharmaceutical solid dosage forms, *Eur. J. Pharm. Biopharm.*, 71 (2009) 2-22.
- [81] C.I. Gioumouxouzis, A. Baklavaridis, O.L. Katsamenis, C.K. Markopoulou, N. Bouropoulos, D. Tzetzis, D.G. Fatouros, A 3D printed bilayer oral solid dosage form

combining metformin for prolonged and glimepiride for immediate drug delivery, *Euro. J. Pharm. Sci.*, 120 (2018) 40-52.

[82] D.M. Smith, Y. Kapoor, G.R. Klinzing, A.T. Procopio, Pharmaceutical 3D printing: Design and qualification of a single step print and fill capsule, *Int. J. Pharm.*, 544 (2018) 21-30.

[83] F. Fina, C.M. Madla, A. Goyanes, J. Zhang, S. Gaisford, A.W. Basit, Fabricating 3D printed orally disintegrating printlets using selective laser sintering, *Int. J. Pharm.*, 541 (2018) 101-107.

[84] A. Krupa, Z. Tabor, J. Tarasiuk, B. Strach, K. Pocięcha, E. Wyska, S. Wroński, E. Łyszczarz, R. Jachowicz, The impact of polymers on 3D microstructure and controlled release of sildenafil citrate from hydrophilic matrices, *Eur. J. Pharm. Sci.*, 119 (2018) 234-243.

[85] A. Goyanes, F. Fina, A. Martorana, D. Sedough, S. Gaisford, A.W. Basit, Development of modified release 3D printed tablets (printlets) with pharmaceutical excipients using additive manufacturing, *Int. J. Pharm.*, 527 (2017) 21-30.

[86] D. Markl, J.A. Zeitler, C. Rasch, M.H. Michaelsen, A. Müllertz, J. Rantanen, T. Rades, J. Bøtker, Analysis of 3D Prints by X-ray Computed Microtomography and Terahertz Pulsed Imaging, *Pharm. Res.*, 34 (2017) 1037-1052.

[87] C. Korte, J. Quodbach, 3D-Printed Network Structures as Controlled-Release Drug Delivery Systems: Dose Adjustment, API Release Analysis and Prediction, *AAPS PharmSciTech*, (2018) (in press) DOI: 10.1208/s12249-018-1017-0.

[88] Y. Wang, D.F. Wertheim, A.S. Jones, A.G.A. Coombes, Micro-CT in drug delivery, *Eur. J. Pharm. Biopharm.*, 74 (2010) 41-49.

[89] Y. Wang, D.F. Wertheim, A.S. Jones, H.I. Chang, A.G.A. Coombes, Micro-CT analysis of matrix-type drug delivery devices and correlation with protein release behaviour, *J. Pharm. Sci.*, 99 (2010) 2854-2862.

[90] A. Krupa, A. Wróbel, O. Cantin, J. Siepmann, B. Strach, E. Wyska, Z. Tabor, R. Jachowicz, In vitro and in vivo behavior of ground tadalafil hot-melt extrudates: How the carrier material can effectively assure rapid or controlled drug release, *Int. J. Pharm.*, 528 (2017) 498-510.

[91] I.S. Russe, D. Brock, K. Knop, P. Kleinebudde, J.A. Zeitler, Validation of terahertz coating thickness measurements using X-ray microtomography, *Mol. Pharm.*, 9 (2012) 3551-3559.

[92] A. Ariyasu, Y. Hattori, M. Otsuka, Non-destructive prediction of enteric coating layer thickness and drug dissolution rate by near-infrared spectroscopy and X-ray computed tomography, *Int. J. Pharm.*, 525 (2017) 282-290.

[93] C. Li, J.A. Zeitler, Y. Dong, Y.C. Shen, Non-destructive evaluation of polymer coating structures on pharmaceutical pellets using full-field optical coherence tomography, *J. Pharm. Sci.*, 103 (2014) 161-166.

[94] U. Bonse, F. Busch, X-ray computed microtomography ( $\mu$ CT) using synchrotron radiation (SR), *Prog. Biophys. Mol. Biol.*, 65 (1996) 133-169.

[95] M. Atsushi, Recent Advances in X-ray Phase Imaging, *Jap. J. App. Phys.*, 44 (2005) 6355.

- [96] L. Wu, M. Wang, V. Singh, H. Li, Z. Guo, S. Gui, P. York, T. Xiao, X. Yin, J. Zhang, Three dimensional distribution of surfactant in microspheres revealed by synchrotron radiation X-ray microcomputed tomography, *Asian J. Pharm. Sci.*, 12 (2017) 326-334.
- [97] L. Fang, X. Yin, L. Wu, Y. He, Y. He, W. Qin, F. Meng, P. York, X. Xu, J. Zhang, Classification of microcrystalline celluloses via structures of individual particles measured by synchrotron radiation X-ray micro-computed tomography, *Int. J. Pharm.*, 531 (2017) 658-667.
- [98] I.C. Sinka, S.F. Burch, J.H. Tweed, J.C. Cunningham, Measurement of density variations in tablets using X-ray computed tomography, *International Journal of Pharmaceutics*, 271 (2004) 215-224.
- [99] V. Busignies, B. Leclerc, P. Porion, P. Evesque, G. Couarraze, P. Tchoreloff, Quantitative measurements of localized density variations in cylindrical tablets using X-ray microtomography, *Eur. J. Pharm. Biopharm.*, 64 (2006) 38-50.
- [100] Deutsches Institut für Normung (DIN) 5031: Strahlungsphysik im optischen Bereich und Lichttechnik, Koblenz, 2013.
- [101] R. Wiedey, P. Kleinebudde, Infrared thermography - A new approach for in-line density measurement of ribbons produced from roll compaction, *Powder Technol.*, 337 (2018) 17-24.
- [102] M.F. Modest, *Radiative Heat Transfer*, Elsevier, 2013.
- [103] L. Boltzmann, Ableitung des Stefan'schen Gesetzes, betreffend die Abhängigkeit der Wärmestrahlung von der Temperatur aus der electromagnetischen Lichttheorie, *Ann. Phys.*, 258 (1884) 291-294.
- [104] W. Wien, Eine neue Beziehung der Strahlung schwarzer Körper zum zweiten Hauptsatz der Wärmetheorie, *Ber. Akad. Wiss. Berlin, Erster Halbband 1893* (1893) 55.
- [105] R. Usamentiaga, P. Venegas, J. Guerediaga, L. Vega, J. Molleda, F.G. Bulnes, Infrared thermography for temperature measurement and non-destructive testing, *Sensors*, 14 (2014) 12305-12348.
- [106] Y.L.Y. R. M. Goody, *Atmospheric Radiation: Theoretical Basis*, Oxford University Press, USA, 1995.
- [107] M. Stricker, Black Body Radiation, *Sun Encyclopedia*, <http://www.sun.org/encyclopedia/black-body-radiation> (accessed June 22<sup>nd</sup>, 2018).
- [108] G. Gaussorgues, Chomet, S., *Infrared Thermography*, Springer Netherlands, 1994.
- [109] K.M. Muckensturm, D. Weiler, F. Hochschulz, C. Busch, T. Geruschke, S. Wall, J. Heß, D. Würfel, R. Lerch, H. Vogt, Measurement results of a 12  $\mu\text{m}$  pixel size microbolometer array based on a novel thermally isolating structure using a 17  $\mu\text{m}$  ROIC, *Proc. SPIE*, 9819 (2016) Article number: 98191N.
- [110] F. Niklaus, A. Decharat, C. Jansson, G. Stemme, Performance model for uncooled infrared bolometer arrays and performance predictions of bolometers operating at atmospheric pressure, *Infrared Phys. Techn.*, 51 (2008) 168-177.
- [111] S.R. Bechard, G.R.B. Down, Infrared imaging of pharmaceutical materials undergoing compaction, *Pharm. Res.*, 9 (1992) 521-528.

- [112] A. Krok, A. Mirtic, G.K. Reynolds, S. Schiano, R. Roberts, C.Y. Wu, An experimental investigation of temperature rise during compaction of pharmaceutical powders, *Int. J. Pharm.*, 513 (2016) 97-108.
- [113] A. Zavaliangos, A. Marx, J. Cunningham, D.A. Winstead, Temperature evolution during compaction of powders, in: 2007 International Conference on Powder Metallurgy and Particulate Materials, PowderMet 2007, Denver, CO, 2007, pp. 136-149.
- [114] A. Zavaliangos, S. Galen, J. Cunningham, D. Winstead, Temperature evolution during compaction of pharmaceutical powders, *J. Pharm. Sci.*, 97 (2008) 3291-3304.
- [115] G.R. Klinzing, A. Zavaliangos, J. Cunningham, T. Mascaro, D. Winstead, Temperature and density evolution during compaction of a capsule shaped tablet, *Comput. Chem. Eng.*, 34 (2010) 1082-1091.
- [116] H. Emteborg, R. Zeleny, J. Charoud-Got, G. Martos, J. Lüddecke, H. Schellin, K. Teipel, Infrared thermography for monitoring of freeze-drying processes: Instrumental developments and preliminary results, *J. Pharm. Sci.*, 103 (2014) 2088-2097.
- [117] A. Krok, N. Vitorino, J. Zhang, J.R. Frade, C.Y. Wu, Thermal properties of compacted pharmaceutical excipients, *Int. J. Pharm.*, 534 (2017) 119-127.
- [118] J.C. Maxwell, *A Treatise on Electricity and Magnetism*, Dover Publications, New York, 1954.
- [119] J.K. Carson, S.J. Lovatt, D.J. Tanner, A.C. Cleland, Thermal conductivity bounds for isotropic, porous materials, *Int. J. Heat Mass Transf.*, 48 (2005) 2150-2158.

## 2 The density distribution in ribbons from roll compaction

Raphael Wiedey, Peter Kleinebudde

Institute of Pharmaceutics and Biopharmaceutics, Heinrich Heine University,  
Universitaetsstrasse 1, 40225 Duesseldorf, Germany

### 2.1 Pretext

*The following research paper has been published in the year 2017 by the journal Chemie-Ingenieur-Technik in Vol. 89 Issue 8 on pages 1017-1024. In divergence from the original document, the word “relative density” was replaced by “solid fraction” when applicable, to preserve uniformity within this thesis.*

*The concept for the study was composed in collaboration by Raphael Wiedey and Peter Kleinebudde. The study design was developed by Raphael Wiedey and optimized based on the advice of Peter Kleinebudde. Raphael Wiedey performed the experimental work as well as the data analysis and wrote the manuscript. Peter Kleinebudde was responsible for revision of the manuscript.*

#### **Evaluation of the authorship:**

author	idea [%]	study design [%]	experimental [%]	evaluation [%]	manuscript [%]
Raphael Wiedey	40	70	100	100	80
Peter Kleinebudde	60	30	0	0	20

## **The density distribution in ribbons from roll compaction**

---

*Raphael Wiedey, Peter Kleinebudde*

*Institute of Pharmaceutics and Biopharmaceutics,*

*Heinrich Heine University Duesseldorf, Germany*

*Chem. Ing. Techn. 89 (2017) 1017-1024*

---

### **Abstract**

The most important quality attribute in roll compaction/dry granulation is the ribbon solid fraction, as it predominantly determines the granule solid fraction and granule size distribution. The solid fraction however, is not distributed homogeneously over the ribbon. In this study, the solid fraction distribution has been investigated using X-Ray micro-computed tomography and demonstrated that characteristic distribution patterns exist over all three spatial directions, the ribbon length, width, and thickness. In detail the distribution patterns depend on the sealing system.

### 3 How relevant is ribbon homogeneity in roll compaction and can it be influenced?

#### 3.1 Pretext

*The following research paper has been published in the European Journal of Pharmaceutics and Biopharmaceutics in Vol. 133 on pages 232-239.*

*Raphael Wiedey was responsible for the idea as well as well as for the study design. He conducted the manufacturing of samples and parts of the characterization thereof and the data evaluation. Raphael Wiedey was furthermore responsible for the manuscript. Rok Šibanc was responsible for parts of the data evaluation. He developed the software that was used for data analysis. Annika Wilms was responsible for parts of the sample characterization as well as the data evaluation. Peter Kleinebudde participated in the development of the idea, gave helpful advice for the study design and was responsible for revision of the manuscript.*

#### Evaluation of the authorship:

author	idea [%]	study design [%]	experimental [%]	evaluation [%]	manuscript [%]
Raphael Wiedey	80	80	80	60	80
Rok Šibanc	0	0	0	30	0
Annika Wilms	0	0	20	10	0
Peter Kleinebudde	20	20	0	0	20

## **How relevant is ribbon homogeneity in roll compaction and can it be influenced?**

*Raphael Wiedey, Rok Šibanc, Annika Wilms, Peter Kleinebudde*

*Institute of Pharmaceutics and Biopharmaceutics,*

*Heinrich Heine University Duesseldorf, Germany*

*Eur. J. Pharm. Biopharm. 133 (2018) 232-239*

---

### **Abstract**

A homogeneous distribution of solid fraction in ribbons is generally assumed to be beneficial during roll compaction/dry granulation. Numerous attempts have been made to increase this homogeneity by modification of the machine, i.e. the roll design and the design of the feeding unit. It has however not been critically tested how relevant this homogeneity really is during subsequent processing. This study investigated two resulting questions: How can process parameters used to increase homogeneity in ribbons and how relevant is this homogeneity for properties of resulting tablets? For that, a statistically designed experiment was performed and ribbon homogeneity analyzed using X-ray micro-computed tomography. Independent from the sealing system used during manufacturing, larger gap widths led to higher homogeneity. The effect of specific compaction force was strongly dependent on the sealing system. When using the cheek plate system, higher specific compaction forces decreased the ribbon homogeneity, while it had no influence when rim rolls were used. In a subsequent study, ribbons of different homogeneity were milled and the resulting granules compressed to tablets. Tablets from homogeneous and inhomogeneous ribbons showed comparable strength and tablet mass variability. Reduced tabletability from highly densified regions of inhomogeneous ribbons was compensated by higher amounts of fines which originate from the more porous regions of ribbons. It was concluded that the relevance of ribbon homogeneity in roll compaction might generally be overestimated.

## 4 Infrared Thermography - A new approach for in-line density measurement of ribbons produced from roll compaction

### 4.1 Pretext

*The following research paper has been published in the year 2018 by the journal Powder Technology in Vol. 337 on pages 17-24. The print version has not been published to date. The idea was developed by both authors, Raphael Wiedey and Peter Kleinebudde, Peter Kleinebudde gave helpful advice in the study design and for data evaluation of the cooling rates and was responsible for the revision of the manuscript. Raphael Wiedey was responsible for the study design, the experimental work, data evaluation and the manuscript.*

#### **Evaluation of the authorship:**

author	idea [%]	study design [%]	experimental [%]	evaluation [%]	manuscript [%]
Raphael Wiedey	60	90	100	90	80
Peter Kleinebudde	40	10	0	10	20

## **Infrared thermography — A new approach for in-line density measurement of ribbons produced from roll compaction**

---

*Raphael Wiedey, Peter Kleinebudde*

*Institute of Pharmaceutics and Biopharmaceutics,*

*Heinrich Heine University Duesseldorf, Germany*

*Powder Technol. 337 (2018) 17-24*

---

### **Abstract**

The ribbon relative density is one of the key quality attributes during roll compaction/dry granulation, as it primarily determines the granule porosity and granule size distribution. In this study, a new approach to measure the ribbon relative density in-line was investigated. A thermographic camera was used to record freshly produced ribbons as they left the gap. In a first step a principal correlation of the measured ribbon temperature and the ribbon density was proven. Furthermore, the cooling rate after compaction was identified as an additional characteristic that can be used to determine the ribbon density. Interestingly the thermographic images also revealed temperature distributions within the ribbon that could be matched with density distributions measured by X-ray micro-computed tomography. In the following, additional characteristics that are equally important for the practical application as an in-line measuring tool were further investigated. The technique showed short reaction times to changes in the process and in a long term experiment no temperature drift over time could be detected. This study demonstrated the applicability of a thermographic camera as an in-line analytical tool for the determination of ribbon relative density.

## 5 Potentials and limitations of thermography as an in-line tool for determining ribbon solid fraction

### 5.1 Pretext

*The following research paper has been published online in the journal Powder Technology in 2018 (DOI: 10.1016/j.powtec.2018.03.047). The print version will be published in Vol. 341 on pages 2-10.*

*The idea was developed by both authors, Raphael Wiedey and Peter Kleinebudde. Peter Kleinebudde gave helpful advice in the study design and was responsible for revising the manuscript. Raphael Wiedey was responsible for the study design, the experimental work, data evaluation and wrote the manuscript.*

#### **Evaluation of the authorship:**

author	idea [%]	study design [%]	experimental [%]	evaluation [%]	manuscript [%]
Raphael Wiedey	80	80	100	100	80
Peter Kleinebudde	20	20	0	0	20

## **Potentials and limitations of thermography as an in-line tool for determining ribbon solid fraction**

---

*Raphael Wiedey, Peter Kleinebudde*

*Institute of Pharmaceutics and Biopharmaceutics,*

*Heinrich Heine University Duesseldorf, Germany*

*Powder Technol. 341 (2019) 2-10*

---

### **Abstract**

The solid fraction of ribbons is one of the key quality attributes during roll compaction/dry granulation, as it predominantly determines the solid fraction and the size distribution of granules. Thus, the development of an in-line measuring technique for monitoring the solid fraction of ribbons during production is highly desirable. Infrared thermography was recently described to be a potential approach, but was so far only tested for MCC. In this study, the applicability of this technique was tested for a number of fillers with different physical characteristics and mixtures with glidants and lubricants. For each material, ribbons were produced and the in-line determined ribbon temperature correlated with the off-line determined ribbon solid fraction. This data was used as a calibration to predict the solid fraction in subsequent studies with varying process parameters. The results show that the technique is applicable for a range of materials, but limited for materials that tend to excessive sticking on the rolls. When magnesium stearate was used, the temperature was increased drastically. This phenomenon could be attributed to additional heat development within the tamping unit. It is concluded that this technique has promising potentials for a range of materials.

## 6 Laser based thermo-conductometry as an approach to determine ribbon solid fraction off-line and in-line

### 6.1 Pretext

*The following research paper has been published in the year 2018 by the International Journal of Pharmaceutics in Vol. 547 Issues 1-2 on pages 330-337. The idea was developed by all three authors. Raphael Wiedey had the idea to use additional energy input into the ribbon and derive ribbon solid fraction from the thermo-conductivity, Rok Šibanc had the idea to generate the energy input by a laser. Raphael Wiedey was responsible for the study design, did most of the experimental work and data evaluation and wrote the manuscript. Rok Sibanc participated in the study design, the experimental work, and the data evaluation. Peter Kleinebudde gave helpful advice in the study design and was responsible for revision of the manuscript.*

#### **Evaluation of the authorship:**

author	idea [%]	study design [%]	experimental [%]	evaluation [%]	manuscript [%]
Raphael Wiedey	60	50	80	80	80
Rok Šibanc	30	40	20	20	0
Peter Kleinebudde	10	10	0	0	20

## **Laser based thermo-conductometry as an approach to determine ribbon solid fraction off-line and in-line**

---

*Raphael Wiedey, Rok Šibanc, Peter Kleinebudde*

*Institute of Pharmaceutics and Biopharmaceutics,*

*Heinrich Heine University Duesseldorf, Germany*

*Int. J. Pharm. 547 (1-2), (2018), 330-337*

---

### **Abstract**

Ribbon solid fraction is one of the most important quality attributes during roll compaction/dry granulation. Accurate and precise determination is challenging and no in-line measurement tool has been generally accepted, yet. In this study, a new analytical tool with potential off-line as well as in-line applicability is described. It is based on the thermo-conductivity of the compacted material, which is known to depend on the solid fraction. A laser diode was used to punctually heat the ribbon and the heat propagation monitored by infrared thermography. After performing a Gaussian fit of the transverse ribbon profile, the scale parameter  $\sigma$  showed correlation to ribbon solid fraction in *off-line* as well as *in-line* studies. Accurate predictions of the solid fraction were possible for a relevant range of process settings. Drug stability was not affected, as could be demonstrated for the model drug nifedipine. The application of this technique was limited when using certain fillers and working at higher roll speeds. This study showed the potentials of this new technique and is a starting point for additional work that has to be done to overcome these challenges.

## 7 Summary and outlook

This thesis deals with the application of new and innovative analytical methods on pharmaceutical production processes. In detail it is focused on the development of a new in-line measuring technique to monitor the ribbon solid fraction during roll compaction/dry granulation. In the presented approaches, infrared thermography was used to derive information on the ribbon solid fraction from its thermal properties. To develop, critically test, and improve the methods, several studies focusing on various aspects have been performed. They can be divided into two parts: the actual development and testing of the measuring technique and a thorough investigation of the distribution of solid fraction within ribbons. This investigation was necessary to estimate the relevance of developing the measuring technique in a way that also allows monitoring of ribbon homogeneity.

The first part was the visualization and analysis of solid fraction distribution patterns in ribbons by X-ray micro-computed tomography. The distribution was analyzed over all three spatial directions, across the ribbon width, along the ribbon length, and over the ribbon thickness. Concerning the ribbon width, findings from literature were confirmed, but visualized in higher resolution. Regarding the ribbon length, it was shown that not only cheek plates, but also rim rolls lead to characteristic distribution patterns. Fast Fourier transform was used to demonstrate that the patterns are caused by rotation of the tamping auger. A distribution of solid fraction was also found over the ribbon thickness. It was slightly decreased towards the side that was facing the master roll during manufacturing. This could be explained by the fact that roll compaction is a unidirectional compression process, in which the force is exclusively applied by the slave roll.

Based on the knowledge about these distribution patterns, a second study was conducted that aimed on the question how this ribbon homogeneity can be influenced by process parameters – an issue that has not been discussed in literature before. The influence of specific compaction force was highly dependent on the sealing system that was used during production. For cheek plates, higher specific compaction forces led to less homogeneous ribbons, while for the rim roll system no influence was found. The influence of the gap width on the homogeneity was independent from the sealing system in a way that larger gap width led to more homogeneous ribbons. The influence of roll speed seemed to be negligible. This is appreciable, since roll speed is the process parameter that is usually changed to control throughput. The results show that not only the overall solid fraction, but

also the homogeneity is not affected to a relevant extent and the product quality is hence kept constant.

To decide if an in-line measurement tool should not only be able to determine the absolute ribbon solid fraction, but also the distribution, a study was conducted that focused on the relevance of ribbon homogeneity. It was performed using microcrystalline cellulose (MCC) and dibasic calcium phosphate anhydrate (DCPA) as model materials. Ribbons of a range of different overall solid fractions were produced using the two sealing systems to achieve extremes regarding ribbon homogeneity. After milling, the granules were compressed to tablets on a pilot scale rotary press. Interestingly, ribbons of identical solid fraction but different homogeneity led to tablets of comparable strength and mass variability. Only for MCC and at low specific compaction forces, homogeneous ribbons led to slightly stronger tablets. Analysis of granule size distributions as well as tablet compression from sieve cuts of the respective granules indicated that inferior tableability of coarse granules from inhomogeneous ribbons was compensated by increased fractions of fines. It was concluded that the relevance of ribbon homogeneity might generally be overestimated.

Furthermore, the results indicate that ribbon homogeneity has a distorting effect in studies on the mechanistic causes of loss in tableability after roll compaction/dry granulation. This loss is caused partly by particle enlargement and partly by work hardening. Based on this study, it was concluded that the role of particle enlargement is probably overestimated. To accurately distinguish between the effects, ribbon homogeneity should be respected in future studies.

Respecting the findings of the first main part of the work, an analytical set-up was developed to monitor ribbon solid fraction in-line. A thermographic camera was installed into a roll compactor and focused on the ribbon just after it left the gap. In the first tests with MCC as a model material, the temperature profile showed a distribution pattern that depended on the sealing system and could be matched with the solid fraction distribution measured by X $\mu$ CT. Regions of high solid fraction showed increased temperature. The temperature increase was attributed to inner friction of the powder during compaction. Equivalently, the mean ribbon temperature correlated with the overall solid fraction. This correlation was independent from the sealing system that was used during compaction and showed short reaction times that would allow real-time monitoring. The results of this

preliminary trial indicated the potential to determine ribbon solid fraction in-line with low instrumental effort.

In a subsequent study, the new approach was tested regarding its suitability in an actual manufacturing environment. The focus was especially on the robustness of the measuring signal towards external influences and the predictive potential of the technique. Correlation between temperature and solid fraction was demonstrated for several further fillers. The differences in slope and offset were however substantial so that a separate calibration would have to be performed for each material. A negative correlation was found between the coefficient of determination of the calibration and the tendency of the material to adhere to the rolls. The suitability might thus be limited for heavily sticking materials. Addition of magnesium stearate to the powder blend led to substantially increased ribbon temperatures. Since the torque of the tamping auger was increased for these experiments, it was hypothesized that this additional input of thermal energy is caused by this unit. Lubrication decreases the friction between powder and roll and by that decreases the nip angle. It was assumed that during these experiments, powder accumulated in the feeding unit, which caused an increased friction between tamping auger and powder. This hypothesis was supported by experiments using rolls with knurled surface in which no increased ribbon temperature could be detected. When fumed silica was added, no increase of temperature was found when compared to pure MCC.

The predictive potential was tested by applying the calibration curves obtained by experiments using different specific compaction forces on ribbons produced at constant SCF, but different gap width. The predictions were accurate over a wide range of gap widths and failed only for ribbons produced at the smallest investigated gap width. Presumably, the ratio between ribbon volume and contact area was so high at these extreme settings that the ribbons had already cooled to a substantial degree when being recorded by the thermographic camera. Apart from these extreme settings however, the measurement seemed to be robust towards changes or fluctuations in process parameters. It also showed that the signal really correlated to the solid fraction and not only to the applied specific compaction force. For binary mixtures of MCC and magnesium stearate, the predictions failed and a separate calibration would have to be performed for each gap width. A PAT tool for monitoring the ribbon solid fraction is especially relevant to detect changes in the product, even though process parameters are kept constant. To test this ability, the climatic conditions, which are known to affect the product quality, were varied. For the model

materials MCC and DCPA, the influence of room temperature and relative humidity on the measurement signal was tested. Both factors had a statistically significant effect on the measurement, which could however be eliminated by referencing the ribbon temperature to the temperature of the rim. By that it could be demonstrated for the first time (in this field) that a PAT tool had an additional value to the sheer monitoring of process parameters.

The final part of this study was a test for stability over process time. Over the course of 60 min, the ribbon temperature increased while the solid fraction stayed constant. As the roll compactor heated up over process time, also the ribbon temperature increased. This drift could not be corrected by referencing to the rim temperature.

To increase robustness towards environmental conditions, the thermal behavior of the ribbons was studied in a more complex way. During the preliminary study, it was observed that the cooling behavior after compaction also depended on the solid fraction. Interestingly, when cheek plates were used, the cooling rate decreased with higher solid fractions, while the trend was inverted when rim rolls were applied. This difference was attributed to the different mechanism of heat transfer during cooling. Cheek plate ribbons are hanging in free air after compaction and mainly cool by convection. In this case, the cooling is predominantly determined by the heat capacity of the ribbon, which increases with higher solid fraction. Highly densified ribbons, with a high heat capacity, cooled down at a lower rate than porous ones. Rim rolls ribbons on the other hand stay in contact with the master roll and are hence mainly cooling by conduction. Conductivity in turn increases with higher solid fraction, leading to a higher cooling rate. These measurements were however not suitable for in-line application, as they were performed by stopping the roll compactor in the process and observing the ribbon temperature in the following. A translation to in-line application was not successful, due to insufficient sensitivity.

It was hypothesized that an increased sensitivity could be enabled by increasing the initial ribbon temperature and by that the difference to the environment temperature. With more pronounced temperature gradients, different cooling behavior caused by different solid fractions would be easier detectable. To achieve this additional energy input, a device containing a 450 nm laser diode was constructed and installed into the roll compactor. It induced a punctual heating of the ribbon surface, which was recorded by the thermographic camera. The temperature profile across the hot-spot could be described accurately by a Gaussian fit. After heating, the heat spread within the ribbon, leading to a broadening of

the cross profile, which could be quantified as the parameter  $\sigma$  of the Gaussian function. The rate at which  $\sigma$  increased correlated to the solid fraction of ribbons. This was principally demonstrated off-line as well as in-line. During in-line experiments, a suitable correlation was only found at low roll speeds. At higher roll speeds, it seems that the exposure time was not sufficient to allow adequate heating. In preliminary tests, it was found that different environmental temperatures could be compensated by referencing the  $\sigma$  value at any given time to the value at which heating ended. Also in-line, no drift of the measured signal could be detected as the roll compactor heated up. Temperature increase of the diode however, which occurred if the laser was switched on permanently, resulted in a decreased laser power and a drift in the signal. It was furthermore demonstrated that the signal shows robustness towards varying gap widths and allows precise and accurate predictions. For two more fillers on which this set-up was tested, the measurements failed. For lactose and DCPA, it was not possible to reach a sufficient heating within the limited exposure time. Transmission measurements demonstrated that laser absorption in these materials was orders of magnitude lower than it was for MCC. The absorption and hence the applicability of the method might be different at other wavelengths.

To investigate, if drug stability issues might be caused by the additional input of thermal and luminous energy, the newly developed system was applied to the model drug nifedipine. In this study, concentration limits for degradation products given by the United States Pharmacopeia were not exceeded. Since nifedipine is known to be extremely photo-sensitive and shows its highest sensitivity at the wavelength range which was used in the set-up, it was concluded that the results can be transferred to most other drugs as well.

It has been demonstrated that infrared thermography has the potential to be a valuable tool for in-line determination of ribbon solid fraction. The approach is cheap, easily implemented into a machine, and does not require extensive chemometric analysis. It is sensitive for a range of materials, has predictive potential, and is robust towards changes in process parameters and climatic conditions. It is furthermore possible to monitor ribbon homogeneity, even though the relevance of this feature is shown to be questionable. Limitations seem to be given, if internal lubrication is applied and by heating of the machine over process time. Robustness regarding this point could be improved by constructing a laser-based system, which derives the ribbon solid fraction from its thermo-conductivity. To make this system applicable for a broader range of materials, a systematic screening for a more suitable wavelength is required. Furthermore, a constant laser power has to be

ensured, either by control mechanisms or by active cooling. To make the system more sensitive at higher roll speeds, either higher laser powers or longer exposure times should be tested. The latter one could be carried out by applying multiple lasers that are focus on successional points on the ribbon, or lasers generating oblong spots.

A final evaluation of the newly developed techniques would require a systematic comparison study with other techniques described in literature – especially NIR spectroscopy. In such a comparison study, the precision, accuracy, sensitivity, and robustness should be tested, as well as the question, if all techniques really give additional information when compared to a monitoring of process parameters.

## 8 Zusammenfassung und Ausblick

Diese Dissertation beschäftigt sich mit der Anwendung neuer und innovativer analytischer Methoden auf pharmazeutische Herstellungsprozesse. Konkret behandelt sie die Entwicklung einer neuen in-line-Messmethode zur Überwachung der Schülpenporosität während des Walzenkompaktierens. Bei den vorgestellten Ansätzen wurde Information über die Schülpenporosität aus dem thermischen Verhalten der Schülpen gezogen. Dafür wurde die Temperatur der Schülpe mittels Infrarot-Thermografie aufgenommen und analysiert. Um die Methode zu entwickeln, kritisch zu testen und weiter zu verbessern, wurden zahlreiche Untersuchungen mit verschiedenem Fokus vorgenommen. Diese können in zwei Teile geteilt werden: die eigentliche Entwicklung und Testung der Messmethode sowie eine gründliche Untersuchung der Porositätsverteilung innerhalb der Schülpe. Diese Untersuchung war notwendig, um die Relevanz der Schülpenhomogenität abzuschätzen und zu entscheiden, ob die neue Methode so entwickelt werden muss, dass auch eine Überwachung der Homogenität möglich ist.

Das erste Kapitel behandelt die Messung und Analyse der Porositätsverteilung in Schülpen, durchgeführt mittels Mikro-Computertomografie. Die Verteilung wurde über alle drei Raumrichtungen – die Schülpenbreite, die Schülpenlänge und die Schülpendicke – untersucht. Bezüglich der Schülpenbreite konnten literaturbekannte Verteilungen bestätigt und in höherer räumlicher Auflösung dargestellt werden. Was die Verteilung entlang der Schülpenlänge angeht, konnte nachgewiesen werden, dass nicht nur bei Benutzung der Herzstückabdichtung, sondern auch bei der Kragenabdichtung charakteristische Verteilungsmuster entstehen. Durch Schnelle-Fourier-Transformation konnte nachgewiesen werden, dass diese periodischen Muster durch die Rotation der Stopfschnecke verursacht werden. Auch über die Schülpendicke konnte eine Verteilung der Porosität festgestellt werden. Auf der Seite, die während der Produktion zur festen Walze gerichtet war, war die Porosität leicht erhöht. Dies konnte plausibel erklärt werden, da die Walzenkompaktierung ein unsymmetrischer Verdichtungsprozess ist, bei dem die Kraft ausschließlich durch die bewegliche Walze ausgeübt wird.

Ausgehend vom Wissen über besagte Porositätsverteilungen, wurde im zweiten Kapitel untersucht wie die Schülpenhomogenität durch Variation der Prozessparameter beeinflusst werden kann. Der Einfluss der spezifischen Kompaktierkraft hing stark vom verwendeten Abdichtungssystem ab. Wenn die Herzstückabdichtung benutzt wurde, führte eine

Erhöhung der spezifischen Kompaktierkraft zu Schülpen mit verringerter Homogenität. Wurde hingegen die Kragenabdichtung benutzt, konnte kein Einfluss auf die Homogenität festgestellt werden. Unabhängig vom Abdichtungssystem führte eine Erhöhung der Spaltbreite zu homogeneren Schülpen. Der Einfluss der Walzengeschwindigkeit auf die Schülpenhomogenität schien hingegen vernachlässigbar zu sein. Dies ist von Vorteil, da über die Walzengeschwindigkeit üblicherweise der Durchsatz geregelt wird. Dadurch wird neben der Gesamtporosität auch deren Verteilung nicht in relevantem Maße verändert und die Produktqualität daher konstant gehalten.

Um zu entscheiden, ob ein Messinstrument für die in-line-Bestimmung der Schülpenporosität auch die Porositätsverteilung erfassen sollte, wurde in der Folge die Relevanz der Homogenität für nachfolgende Prozessschritte überprüft. Dafür wurden mikrokristalline Cellulose (MCC) und kristallwasserfreies Calciumhydrogenphosphat (DCPA) als Modellsubstanzen gewählt. Schülpen verschiedener Porosität wurden hergestellt und durch Verwendung der verschiedenen Abdichtungssysteme Extreme hinsichtlich der Homogenität erreicht. Nach dem Granulierschritt wurden die erhaltenen Granulate tablettiert und charakterisiert. Überraschenderweise führten die Granulate aus homogenen und inhomogenen Schülpen bei gleicher Gesamtporosität zu Tabletten mit vergleichbarer Festigkeit und Massenvariation. Nur für MCC wurde bei niedrigen spezifischen Kompaktierkräften eine leichte Überlegenheit der homogenen Schülpen hinsichtlich der Tablettenfestigkeit festgestellt. Eine Analyse der Granulatgrößenverteilung sowie das Verpressen von Siebfractionen zu Tabletten deuteten darauf hin, dass die reduzierte Wiederverpressbarkeit von groben Granulatkörnern aus inhomogenen Schülpen durch gleichzeitig auftretende erhöhte Feianteile kompensiert wurde. Da weder hinsichtlich der Tablettenfestigkeit, noch hinsichtlich der Massenvariabilität relevante Unterschiede festgestellt wurden, wurde geschlossen, dass die Relevanz der Schülpenhomogenität generell überbewertet ist.

Weiterhin hat die Porositätsverteilung einen verfälschenden Effekt auf Untersuchungen der mechanistischen Ursachen der reduzierten Wiederverpressbarkeit nach Walzenkompaktieren/Trockengranulieren. Dieser Verlust wird zum Teil durch Partikelvergrößerung und zum Teil durch *work hardening* erklärt. Aufgrund der vorliegenden Daten wurde geschlossen, dass die Rolle der Partikelvergrößerung überbewertet ist. Um akkurat zwischen den Effekten unterscheiden zu können, muss die Schülpenhomogenität in zukünftigen Arbeiten berücksichtigt werden.

Auf Grundlage der Ergebnisse des ersten Hauptteils der Arbeit wurde in der Folge ein analytisches Gerät entwickelt um die Schülpenporosität in-line zu messen. Eine thermografische Kamera wurde in einen Walzenkompaktor eingebracht und auf die Schülpe direkt unterhalb des Spaltes fokussiert. In ersten Untersuchungen mit der Modellsubstanz MCC wurde eine Temperaturverteilung innerhalb der Schülpe gefunden die vom verwendeten Abdichtungssystem abhing und mit der Porositätsverteilung übereinstimmte. Regionen geringer Porosität zeigten erhöhte Temperaturen. Der Temperaturanstieg wurde mit der inneren Reibung des Pulvers während der Verdichtung erklärt. Dementsprechend korrelierte auch die mittlere Temperatur der Schülpe negativ mit ihrer Porosität. Diese Korrelation war unabhängig vom Abdichtungssystem und auch die Reaktionszeit nach Änderung der Prozessparameter war kurz. Daher ist der Ansatz die Schülpenporosität aus der Temperatur zu schließen vielversprechend.

In der Folge wurde der neue Ansatz auf die tatsächliche Eignung im Umfeld der pharmazeutischen Produktion getestet. Der Fokus lag dabei besonders auf der Robustheit des Messsignals gegenüber äußeren Einflüssen und der Fähigkeit der Methode Vorhersagen zu treffen. Die Korrelation zwischen Temperatur und Porosität wurde für diverse weitere Füllstoffe gezeigt. Dabei waren die Unterschiede in Steigung und Achsenabschnitt jedoch substanziell, sodass für jedes Material eine separate Kalibrierung notwendig wäre. Dabei wurde eine negative Abhängigkeit der Güte der Korrelation von der Tendenz des Materials an den Walzen anzuhaften gefunden. Die Eignung der Methode könnte deshalb bei stark adhärierenden Materialien begrenzt sein. Der Zusatz von Magnesiumstearat bewirkte eine deutliche Erhöhung der Schülpentemperaturen. Da das Drehmoment der Stopfschnecke während des Prozesses um ein Vielfaches erhöht war, wurde angenommen, dass der zusätzliche Eintrag thermischer Energie durch dieses Bauteil zustande kam. Schmiermittel setzen unter anderem die Reibung zwischen Pulver und Walze herab, dadurch wurde in diesen Versuchen der Einzugswinkel reduziert und das Pulver in der Fördereinheit zurückgestaut. Der erhöhte Füllstand sorgte für erhöhte Reibung zwischen Stopfschnecke und Pulver und damit auch für erhöhte Temperaturen. Diese Hypothese wurde durch Experimente mit geriffelten Walzen gestützt, bei denen im Vergleich zu MCC keine erhöhte Schülpentemperatur gefunden wurde. Der Zusatz von kolloidaler Kieselsäure hatte keinen vergleichbaren Effekt wie Magnesiumstearat und führt nicht zu zusätzlich erhöhten Temperaturen.

Die Fähigkeit der Messtechnik richtige Vorhersagen der Schülpenporosität zu machen wurde getestet, indem die Daten aus Experimenten mit verschiedenen spezifischen Kompaktierkräften als Kalibrierung auf Experimente angewendet wurden, bei denen die Kompaktierkraft konstant gehalten, aber die Spaltbreite variiert wurde. Die Vorhersagen zeigten akzeptable Präzision und Richtigkeit über einen weiten Bereich von Spaltbreiten. Nur für die geringste untersuchte Spaltbreite wichen die Vorhersagen signifikant von den Referenzwerten ab. Bei diesem Versuch war das Verhältnis von Schülpenvolumen zu Kontaktfläche mit der Walze so gering, dass eine Abkühlung der Schülpe stattfinden konnte noch bevor die Temperatur durch die Infrarotkamera bestimmt werden konnte. Abgesehen von diesem Extrempunkt schien die Messmethode robust gegen Variation und Fluktuation der Spaltbreite während des Prozesses zu sein. Das Messsignal korrelierte mit der Schülpenporosität und nicht etwa nur mit der ausgeübten spezifischen Kompaktierkraft. Für binäre Mischungen aus MCC und Magnesiumstearat schlugen die Vorhersagen mit dieser Methode fehl. In diesem Fall müsste daher für jede Spaltbreite eine separate Kalibrierung aufgenommen werden.

Um zu testen, ob die in-line-Messungen Informationen zur Produktqualität liefern können, die über eine Überwachung der Prozessparameter hinausgehen, wurde Bedingungen simuliert bei denen trotz identischer Prozesseinstellungen unterschiedliche Produkteigenschaften zu erwarten waren. Dazu wurde für die Modellmaterialien MCC und DCPA die Robustheit der Messmethode gegenüber Veränderungen der Raumtemperatur und der relativen Luftfeuchte getestet. Beide Faktoren hatten einen statistisch signifikanten Einfluss auf das Messergebnis. Dieser Einfluss konnte jedoch durch Referenzierung der Schülpentemperatur auf die Temperatur des Walzenkragens eliminiert werden. Es ist das erste Mal, dass für ein PAT-Messinstrument in dieser Fragestellung gezeigt werden konnte, dass es Informationen zur Produktqualität liefert, die sich aus der Überwachung der Prozessparameter nicht ziehen ließen.

Der letzte Teil dieser Messreihe war die Untersuchung der Stabilität des Messsignals über die Prozesszeit. Während einer Dauer von 60 min erhöhte sich die Schülpentemperatur, während die Schülpenporosität konstant blieb. Durch das Aufheizen des Walzenkompaktors über die Prozesszeit erhöhte sich auch die Schülpentemperatur. Diese Abweichung konnte auch durch Referenzierung gegen die Kragentemperatur nicht kompensiert werden.

Um die Robustheit gegenüber externen Einflüssen, besonders der Maschinentemperatur, zu erhöhen, wurde das thermische Verhalten der Schülpen weitergehend untersucht. Während der vorhergehenden Studie wurde beobachtet, dass auch das Abkühlverhalten der Schülpen von der Porosität abhing. Interessanterweise war die Abhängigkeit von Porosität und Abkühlverhalten für die beiden Abdichtungssysteme unterschiedlich. Schülpen die mit der Herzstückabdichtung hergestellt wurden, zeigten umso höhere Abkühlraten, je poröser sie waren, während die Korrelation bei Kragenschülpen umgekehrt war. Dieser Unterschied wurde den unterschiedlichen Mechanismen des Wärmeübergangs zugeschrieben. Herzstückschülpen hängen nach Verlassen des Spalts frei in der Luft und kühlen vorwiegend über Konvektion. In diesem Fall hing die Rate des Abkühlens im Wesentlichen von der Wärmekapazität der Schülpe ab, die mit höherer Porosität kleiner ist. Stark verdichtete Schülpen mit niedriger Porosität und hoher Wärmekapazität kühlten entsprechend langsamer ab. Kragenschülpen hingegen bleiben nach Verlassen des Spaltes im Kontakt mit der festen Walze und kühlen dementsprechend vorwiegend durch Konduktion. Die Wärmeleitfähigkeit wiederum steigt mit hohem Feststoffanteil, also niedriger Porosität, an. Hochverdichtete Schülpen mit hoher Leitfähigkeit kühlten folglich am schnellsten ab. Diese Messungen des Abkühlverhaltens waren jedoch nicht geeignet für eine in-line-Anwendung, da sie durch Stoppen des Walzenkompaktors im Prozess und anschließendes Verfolgen der Schülpentemperatur durchgeführt wurden. Der Versuch einer Übertragung in den laufenden Betrieb war aufgrund mangelnder Empfindlichkeit nicht erfolgreich.

Es wurde die Hypothese aufgestellt, dass die Empfindlichkeit durch das Erreichen höherer Ausgangstemperaturen der Schülpen erhöht werden könne. Bei höheren Temperaturdifferenzen der Schülpe zu ihrer Umgebung müssten unterschiedliche Abkühlraten leichter zu detektieren sein. Um diesen zusätzlichen Energieeintrag zu generieren, wurde eine Anlage konstruiert, die eine 450 nm Laserdiode enthält und einfach in den Innenraum des Walzenkompaktors eingebracht werden konnte. Der Laser induzierte eine punktuelle Erhitzung der Schülpenoberfläche, die mit der Infrarotkamera aufgenommen werden konnte. Das Temperaturprofil durch den erhitzten Punkt konnte durch eine Gaussfunktion angemessen beschrieben werden. Nach dem Erhitzen verteilte sich die Wärme in der Schülpe, was in einer Verbreiterung der Gausskurve resultierte. Diese Verbreiterung konnte als Streuungsparameter  $\sigma$  quantifiziert werden. Die Rate, in der  $\sigma$  während des Abkühlens anstieg, korrelierte negativ mit der Porosität der Schülpe.

Dies wurde sowohl off-line als auch in-line grundlegend gezeigt. Bei den in-line Versuchen wurde eine verwertbare Korrelation nur bei geringen Walzengeschwindigkeiten gezeigt. Bei höheren Geschwindigkeiten schien die Belichtungszeit nicht ausreichend gewesen zu sein um die notwendige Erwärmung der Schülpe zu erlauben. In Vorversuchen konnte gezeigt werden, dass Variationen der Umgebungstemperatur durch Referenzierung von  $\sigma$  während des Abkühlens auf  $\sigma$  beim Ende des Aufheizens ausgeglichen werden konnten. Auch in den in-line Versuchen blieb das Signal stabil, während der Walzenkompaktor sich über die Prozesszeit aufheizte. Eine Erwärmung der Laserdiode jedoch, die auftrat, wenn der Laser längere Zeit am Stück aktiv war, führte zu abnehmender Laserleistung, die wiederum das Signal beeinflusste. Das Signal war stabil gegenüber Variationen der Spaltbreite und erlaubte zutreffende Vorhersagen über die Schülpenporosität. Für DCPA und Laktose, zwei weitere Füllstoffe, mit denen das System getestet wurde, waren keine Messungen möglich. In beiden Fällen konnte der Laser das Material nicht angemessen aufheizen. Transmissionsmessungen zeigten, dass die Absorption der Laserstrahlung bei diesen Materialien Größenordnungen geringer war als bei MCC. Möglicherweise ist die Absorption bei anderen Wellenlängen höher und die Messmethode damit geeigneter.

Zur Überprüfung, ob der zusätzliche Eintrag an Wärme und Lichtenergie die Stabilität des Wirkstoffs einschränken könnte, wurden Versuche mit der Modellsubstanz Nifedipin durchgeführt. Die Grenzwerte der United States Pharmacopeia für Abbauprodukte des Nifedipins wurden dabei deutlich unterschritten. Da Nifedipin hochgradig photoinstabil ist und das Maximum der Lichtempfindlichkeit zudem im gleichen Wellenlängenbereich wie die verwendete Laserstrahlung liegt, wird angenommen, dass sich diese Ergebnisse auf die meisten Arzneistoffe übertragen lassen.

Infrarotthermografie hat das Potenzial ein wertvolles Werkzeug zur Überwachung der Schülpenporosität zu sein. Der Ansatz ist kostengünstig, einfach in bestehende Produktionsanlagen implementierbar und benötigt keine aufwändige chemometrische Datenanalyse. Er ist sensitiv für eine Spannweite an Materialien, erlaubt Vorhersagen und ist robust gegenüber Änderungen der Prozessparameter und klimatischen Bedingungen. Es ist die einzige Messmethode zur Überwachung der Schülpenporosität, bei der einerseits kritische Robustheitsstudien durchgeführt wurden und andererseits gezeigt werden konnte, dass die Messungen Informationsgehalt haben, der über den der aufgezeichneten Prozessparameter hinausgeht. Es ist weiterhin möglich auch die Schülpenhomogenität zu überwachen, obschon gezeigt werden konnte, dass die Relevanz dieser Eigenschaft fraglich

ist. Einschränkungen scheinen bei der Verwendung von Schmiermittel und durch die Erhitzung der Maschine über die Prozesszeit gegeben zu sein. Robustheit gegenüber dieser Erhitzung konnte durch die Entwicklung eines neuen, Laser-basierten Analysegerätes verbessert werden, bei dem die Porosität aus der Wärmeleitfähigkeit der Schülpen bestimmt wird. Um diese verbesserte Methode für eine breitere Auswahl an Materialien möglich zu machen, ist in zukünftigen Arbeiten eine systematische Untersuchung geeigneter Wellenlängen notwendig. Des Weiteren muss eine konstante Laserleistung sichergestellt werden. Dies könnte entweder durch Regelungsmechanismen oder durch aktive Kühlung geschehen. Um die Empfindlichkeit auch bei höheren Walzengeschwindigkeiten auf ein ausreichendes Maß zu heben, könnten entweder höhere Laserleistungen oder längere Belichtungszeiten getestet werden. Letzteres wäre zum Beispiel durch die Installation mehrerer Laserdioden möglich, die auf aufeinanderfolgende Punkte der Schülpe fokussiert sind, oder durch die Verwendung von Lasern mit länglichem Fokus.

Für eine abschließende Bewertung der neuen Messmethoden bedarf es eines systematischen Vergleichs mit anderen literaturbekannten Messmethoden, insbesondere der NIR-Spektroskopie. In einer solchen Vergleichsstudie müssten neben Präzision, Richtigkeit und Empfindlichkeit auch die Robustheit getestet werden und ob alle Messmethoden einer reinen Überwachung der Prozessparameter wirklich überlegen sind.

## 9 List of original publications

1. Raphael Wiedey, Peter Kleinebudde  
Density distribution in ribbons from roll compaction  
*Chem. Ing. Techn.* 89 (2017) 1017-1024
2. Raphael Wiedey, Peter Kleinebudde  
Infrared thermography - A new approach for in-line density measurement of ribbons produced from roll compaction  
*Powder Technol.* 337 (2018) 17-24
3. Kitti Csordas, Raphael Wiedey, Peter Kleinebudde  
Impact of roll compaction design, process parameters, and material deformation behaviour on ribbon relative density  
*Drug. Dev. Ind. Pharm.* 44 (2018) 1295-1306
4. Raphael Wiedey, Rok Sibanc, Peter Kleinebudde  
Laser based thermo-conductometry as an approach to determine ribbon solid fraction off-line and in-line  
*Int. J. Pharm.* 547 (2018) 330-337
5. Raphael Wiedey, Rok Sibanc, Annika Wilms, Peter Kleinebudde  
How relevant is ribbon homogeneity in roll compaction/dry granulation and how can it be influenced?  
*Eur. J. Pharm. Biopharm.* 133 (2018) 232-239
6. Raphael Wiedey, Peter Kleinebudde  
Potentials and limitations of thermography as an in-line tool for determining ribbon solid fraction  
*Powder Technol.* 341 (2019) 2-10

## 10 Contributions to meetings

### 10.1 Oral presentations

1. Raphael Wiedey, Peter Kleinebudde  
Characterization of Ribbon Density by X-Ray Micro-Computed Tomography and IR Camera  
*10<sup>th</sup> Annual PSSRC Symposium, Kopenhagen, 2016*
2. Raphael Wiedey, Peter Kleinebudde  
How do process parameters influence the density distribution in ribbons from roll compaction?  
*2<sup>nd</sup> European Conference on Pharmaceutics, Kraków, 2017*
3. Raphael Wiedey, Peter Kleinebudde  
In-line determination of ribbon solid fraction by thermographic camera  
*8<sup>th</sup> International Granulation Workshop and Conference, Sheffield, 2017*

### 10.2 Poster presentations

1. Raphael Wiedey, Peter Kleinebudde  
Kinetics of tablet over-lubrication determined by the capillary rise method  
*10<sup>th</sup> PBP World Meeting, Glasgow, 2016*
2. Raphael Wiedey, Peter Kleinebudde  
Is ribbon homogeneity important?  
*9<sup>th</sup> Polish-German Symposium on Pharmaceutical Sciences, Krakow, 2017*
3. Raphael Wiedey, Peter Kleinebudde  
Material dependence in the applicability of thermographic measurements for in-line monitoring of ribbon solid fraction  
*AAPS Annual Meeting and Exposition, San Diego, 2017*
4. Raphael Wiedey, Annika Wilms, Peter Kleinebudde  
How relevant is ribbon homogeneity in roll compaction/dry granulation?  
*11<sup>th</sup> PBP World Meeting, Granada, 2018*

## 11 Danksagung

Herzlicher Dank gilt zuerst meinem Doktorvater Prof. Dr. Dr. h.c. Peter Kleinebudde für die Aufnahme in seine Arbeitsgruppe und die Betreuung, die ich in dieser Zeit erfahren habe. Sie haben sich immer Zeit genommen, um kurzfristig Abstracts zu korrigieren, Ergebnisse zu besprechen oder spontan Verträge zu verlängern. Ich möchte mich für das vermittelte Fachwissen bedanken, noch mehr jedoch für das Vermitteln wissenschaftlicher Methodik. Herrn Prof. Dr. Jörg Breitreutz möchte ich für die Übernahme des Koreferats danken und besonders auch für fachliche Gespräche und Diskussionen, die über den Inhalt dieser Dissertation hinausgingen. Beiden Professoren möchte ich zudem für das Ermöglichen zahlreicher Konferenzreisen danken. Diese haben mir gleichermaßen Freude und Wissen vermittelt und meinen Horizont auf unterschiedlichste Weise erweitert.

Rok Šibanc gebührt besonderer Dank für die Hilfe, die er mir bei verschiedensten Problemen geleistet hat. Das gilt für die Entwicklung von Auswertungs-Software, aber ganz besonders dafür, dass er mir gänzlich neue Techniken des Arbeitens und der Datenauswertung nahegebracht hat, ohne die bedeutenden Teile dieser Arbeit nicht möglich gewesen wären. Annika Wilms danke ich für die tatkräftige Unterstützung bei einem der abschließenden Projekte dieser Arbeit. Ebenso möchte ich Veronika Hagelstein von der Friedrich-Wilhelms-Universität Bonn für ihre freundliche Unterstützung bei Tablettiersversuchen danken. Tomas Pioch und Mariele Fligge danke ich für ihren Einsatz während ihres Wahlpflichtpraktikums, in denen Teile der Robustheitsstudie durchgeführt wurden. Dr. Julian Quodbach danke ich für seinen Einsatz bei der Anschaffung des X $\mu$ CT und bei der Beseitigung der vielen Kinderkrankheiten dieses Geräts und dafür, dass er mir die Arbeit mit der Thermographie-Kamera nahegelegt hat. Dr. Klaus Knop danke ich dafür, dass er immer bereit war seine Erfahrung zu teilen und bei den vielen kleinen Problemen, die im Laufe der vergangenen drei Jahre aufgetreten sind, eine große Hilfe war.

Haress Mangal danke ich für die herzliche Aufnahme in sein Büro, die vielen fachlichen und persönlichen Gespräche, Erlebnisse auf Konferenzreisen und vieles mehr. Gleiches gilt für meine weitere Bürokollegin Isabell Speer. Durch euch beide bin ich jeden Tag wieder gerne ans Institut gekommen und wir waren zu Recht als das #besteBüro bekannt!

Simon Grote danke ich für den Spaß und die Erlebnisse die wir in den vergangenen dreieinhalb Jahren im Institut, auf Konferenzen und bei vielen anderen Gelegenheiten

hatten. Carolin Korte danke ich für die kritischen Diskussionen großer und kleiner Fragestellungen, die mit zur Entwicklung dieser Arbeit beigetragen haben. Robin Meier gilt mein Dank, da er mir in seiner Zeit am Institut wertvolle Unterstützung bei meinen ersten Schritten gab. Auch in seiner jetzigen Tätigkeit hat er durchgehend Interesse am Voranschreiten meiner Arbeit gezeigt und mir die Möglichkeit gegeben Versuche im großen Maßstab bei L.B. Bohle in Ennigerloh durchzuführen. Stefan Stich danke ich recht herzlich für seine Bereitschaft technische Probleme durch seine Erfahrung und sein handwerkliches Geschick zu lösen. Auch allen weiteren aktuellen und ehemaligen Mitarbeitern des Institutes, die nicht bisher genannt wurden, danke ich für die angenehme Zeit – insbesondere meinen Walzenkompaktierkollegen und der Prag-Runde.

Zuletzt möchte ich meiner Familie und meinen Freunden bedanken, die mich während der vergangenen Jahre immer unterstützt haben und mir zu jeder Zeit ein fester Rückhalt waren.

## 12 Appendix

### 12.1 General

The following code was written in python 3.5 for the several steps of data analysis in the studies based on laser-based thermo-conductimetry. Comments are indicated by a # symbol and written in italic type. File names that appear in the given code are exemplarily chosen.

### 12.2 Averaging images

```
# import libraries containg functions for data analysis
# pandas: user-friendly work with panel-data
# numpy: numerical analysis
# natsorted: sorting strings by various criteria

import pandas as pd
import numpy as np
import glob
from natsort import natsorted

files = natsorted(glob.glob("*8kN2mm.txt"))

averageby = 56

for i,file in enumerate(files):
    if i%averageby == 0:
        df = pd.read_csv(file,sep=";",header=None)
    else:
        df += pd.read_csv(file,sep=";",header=None)
    print(i)

    if i%averageby == averageby-1:
        df /= averageby

df.to_csv("avg_8kN2mm2rpm_{}.txt".format(i),header=None,index=None)
```

### 12.3 Gaussian fit row-wise

```
# read csv, fit gauss over row and write sigma to new csv
# pandas: user-friendly work with panel-data
# numpy: numerical analysis
# scipy: library containing many functions für data analysis, e.g. curve fitting

import pandas as pd
import numpy as np
from scipy.optimize import curve_fit
import matplotlib.pyplot as plt
import glob

filename = "10kN2mm.txt"

# define Gauss function

def gauss(x,loc,sigma,a,b):
    return a*((1/((2*np.pi*sigma**2)**0.5))*(np.exp**(((x-loc)**2)/
(2*sigma**2))))+b

def fit(filename):

    df = pd.read_csv(filename,sep=",",decimal=".",header=None) #read data from csv

    data = []

    x = np.arange(df.shape[1]-1)
    xfit = np.linspace(0,x[-1],100)

    p0=[40,10,150,23] # starting values for fit parameters

    for i in range(df.shape[0]):
        print(i)
```

```
y = df.iloc[i,1:].as_matrix()
#popt, pcov = curve_fit(gauss,x,y)
try:
    pop, pcov = curve_fit(gauss,x,y,p0)
    data.append([df.iloc[i,0]]+list(pop))
except:
    data.append([df.iloc[i,0]]+[0,0,0,0])

if True:
    if i%10 == 0:    # save figure of temperature profile and fitted curve
        try:
            fig, ax = plt.subplots()
            ax.plot(x,y,".")
            yfit = gauss(xfit,*pop)
            ax.plot(xfit,yfit,"-")

            fig.savefig("{}_fit{}.png".format(filename,i))
            plt.close()

        except:
            pass

filename_out = filename.replace(".txt","_fit.csv")
dfout = pd.DataFrame(data,columns=["t","loc","sigma","a","b"])
dfout.to_csv(filename_out, sep=';', index=True)    # save fit parameters in new csv
file

fig, ax = plt.subplots()
dfout.plot.line(x="t",y="sigma",ax=ax)
fig.savefig("sigma_t.png")

filenames = glob.glob('*.*.txt')
print(filenames)
for filename in filenames:
    print(filename)
    fit(filename)
```

## 12.4 Plotting $\sigma$ and amplitude of peaks

```
# import libraries containg functions for data analysis
# pandas: user-friendly work with panel-data
# numpy: numerical analysis
# matplotlib: plotting of data
# glob: selecting files by name

%matplotlib inline
import pandas as pd
import numpy as np
import matplotlib.pyplot as plt
import glob

# select data files that are to be plotted

files = glob.glob("**/*6kN2mm*fit.csv",recursive=True)

plotfiles = [
    [files[:12],"r"]

]

# create new dataframe to save fit coefficients in

newdata = pd.DataFrame()

fig1, ax1 = plt.subplots(figsize=(20,12))
fig2, ax2 = plt.subplots(figsize=(20,12))

for files,c in plotfiles:
    for file in files:
        df = pd.read_csv(file,sep=";",index_col=0)
        df["amp"] = df["a"]/((2*np.pi*df["sigma"]**2)**0.5) # calculate amplitude
        df["sigma"] = df["sigma"].abs()
```

```
istart = df["amp"].idxmax()
dfp = df.loc[istart:]
dfp.reset_index(inplace=True)

label = file[8:14]

dfp.plot(y="amp",ax=ax1,label=label,c=c)
dfp.plot(y="sigma",ax=ax2,label=label,c=c)
filename_out = file.replace(".csv","_new.csv")
dfp.to_csv(filename_out)
newdata[file] = dfp['sigma']
ax1.set_ylim(0,15)
ax1.set_xlim(0,150)
ax2.set_ylim(4,14)
ax2.set_xlim(0,300)

ax1.set_xlabel("px")
ax1.set_ylabel("amplitude [K]")

ax2.set_xlabel("px")
ax2.set_ylabel("sigma [px]")

newdata.to_csv('overview.csv', sep=";")

fig1.savefig('amplitude.png')
fig2.savefig('sigma.png')
```

## **Erklärung**

Ich versichere an Eides Statt, dass die Dissertation von mir selbständig und ohne unzulässige fremde Hilfe unter Beachtung der „Grundsätze zur Sicherung guter wissenschaftlicher Praxis an der Heinrich-Heine-Universität Düsseldorf“ erstellt worden ist.

Raphael Wiedey